URBAN CLIMATE/ METEOROLOGY SESSIONS

RESULTS OF ANALYSIS OF SONIC ANEMOMETER OBSERVATIONS AT STREET LEVEL AND AT ROOFTOP IN MANHATTAN
Steven Hanna and Ying Zhou - Harvard School of Public Health, Boston, Massachusetts USA

QUASI-STEADY STATE EQUILIBRIUM BOUNDARY LAYER HEIGHT DETERMINATION IN URBAN CONDITIONS
Amela Jeričević - Croatian Meteorological and Hydrological Service, Grič 3, 10000 Zagreb, Croatia

RELATIONSHIPS BETWEEN AIR POLLUTION AND METEOROLOGY IN NEWCASTLE, AUSTRALIA
Howard Bridgman and James O'Connor - School of Environmental and Life Sciences, University of Newcastle NSW 2308 Australia

AN INTERCOMPARISION OF DIAGNOSTIC URBAN WIND FLOW MODELS BASED ON THE RÖCKLE METHODOLOGY USING THE JOINT URBAN 2003 FIELD DATA
Steven Hanna[1], John White[2], John Hannan[3], Ronald Kolbe[4], Christopher Kiley[4], Michael Brown[5], Thomas Harris[6], Yansen Wang[7], Rick Fry[3], James Bowers[2], Dennis Garvey[7], Chatt Williamson[7], and Jacques Moussifir[8] - [1] Hanna Consultants, Kennebunkport, ME, [2]US Army Test and Evaluation Command, Dugway Proving Ground, UT, [3] US Defense Threat Reduction Agency, Ft Belvoir, VA
[4] Northrop Grumman IT, Lorton, VA, [5] Los Alamos National Laboratory, Los Alamos, NM, [6] Science Applications International Corporation, [7] US Army Research Laboratory, Adelphia, MD, [8] ARIA Technologies, Paris, France

IMPACT OF URBANISATION ON THE SOME ATMOSPHERIC VARIABLES IN AKURE, ONDO STATE, NIGERIA
O. M Akinbode[1], A.O. Eludoyin[2] and O. A. Ediang[3] – [1] Department of Geography and Planning Sciences, Adekunle Ajasin University, Akungba Akoko, Ondo State, [2] Department of Geography, Obafemi Awolowo University, Ile - Ife, Nigeria, [3] Nigerian meteorological agency, Lagos, Nigeria

DEVELOPMENT OF GAMMA-MET ON SENSIBLE HEAT CALCULATION FOR URBAN CHARACTERISTIC: CASE STUDY BANGKOK, THAILAND
Surat Bualert - Faculty of Science, Chulalongkorn University, Bangkok 10330, Thailand

THE MIXING HEIGHT DETERMINATION IN TESTBED CAMPAIGN IN HELSINKI, FINLAND
N. Eresmaa[(1)], A. Karppinen[(1)], K. Bozier[(2)], M. Rantamäki[(1)] - (1) Finnish Meteorological Institute, (2) University of Salford, Great Britain

AIR POLLUTION METEOROLOGY – A CASE STUDY OF SWANSEA, UK
T. Habeebullah[1], S. Dorling[1] and P.Govier[2] - [1] School of Environmental Sciences, University of East Anglia, UK
[2] City and County of Swansea, Environment Department, Swansea, UK

IMPROVING THE MARTILLI'S URBAN BOUNDARY LAYER SCHEME: VALIDATION IN THE BASEL REGION
R. Hamdi[1], G. Schayes - Institut d'Astronomie et de Géophysique George Lemaître, University of Louvain, B-1348 Louvain-la-Neuve, Belgium, [1]present affiliation : Royal Meteorological Institute of Belgium, Uccle, Brussels, Belgium

EVALUATION OF THE PBL MODEL YORDAN WITH COPENHAGEN DATA FOR APPLICATION IN AIR POLLUTION MODELING
M. Kolarova[1], D. Yordanov[2], D. Syrakov[1], T.Tirabassi[3], U. Rizza[4], and C. Mangia[4] - [1] National Institute of Meteorology and Hydrology (NIMH) - BAS, Sofia, BULGARIA, [2] Institute of Geophysics - BAS, Sofia, BULGARIA, [3] ISAC, CNR, Bologna, ITALY, [4] ISAC, CNR, Lecce, ITALY

IMPLEMENTATION AND TESTING OF URBAN PARAMETERIZATION IN THE WRF MESOSCALE MODELING SYSTEM.
Alberto Martilli[1] - CIEMAT, Madrid, Spain. Rainer Schmitz - Universidad de Chile, Santiago, Chile. Fernando Martin - CIEMAT, Madrid, Spain.

Proceedings of the 6th International Conference on Urban Air Quality
Limassol, Cyprus, 27-29 March 2007

RESULTS OF ANALYSIS OF SONIC ANEMOMETER OBSERVATIONS AT STREET LEVEL AND AT ROOFTOP IN MANHATTAN

Steven Hanna* and Ying Zhou
Harvard School of Public Health, Boston, Massachusetts USA, shanna@hsph.harvard.edu

ABSTRACT

The results are presented of analysis of sonic anemometer observations near street-level and at roof-top in Manhattan. The March MSG05 experiment employed five near-surface sites and two roof-top sites on two well-mixed days with moderate winds. The August MID05 experiment employed 10 surface sites and five roof-top sites in an area south of Central Park on six days with light winds. Comparisons are made with similar data from the JU2003 experiment in Oklahoma City. The 30-minute averaged similarity relations (e.g., σ_u/u^*) are fairly consistent from one experiment to another. For example, the local σ_w/u^* is about 1.5 and the local u^*/u is about 0.24. The ratio σ_T/T^* in the street-canyons is about -3, even at night consistent with very-slightly unstable conditions. The σ_u etc at the surface are about 40 % of their values at the rooftops. It is found that the variations across anemometers and from one time period to another are generally less than 50 % of the 30 min averages analyzed above.

1. INTRODUCTION

This paper expands upon the comprehensive analysis by Hanna et al. (2007) of sonic anemometer observations obtained in short-term intensive urban field studies in Oklahoma City (OKC), known as the Joint Urban 2003 (JU2003) experiment, and in Manhattan, known as the Madison Square Garden 2005 (MSG05) experiment. The current analysis adds data from a second field study in Manhattan, known as the Midtown 2005 (MID05) experiment.

Clarke et al. (1987) measured turbulence over St. Louis in the mid-1970's and showed the presence of large increases in the turbulent velocities over the urban area, with the difference accentuated at night. In the past 15 to 20 years, there have been several reviews and analyses of urban wind and turbulence, including those by Rotach (1995) and Roth (2000). Some suggested similarity relations for urban winds and turbulence are listed by Britter and Hanna (2003) and Hanna et al. (2007). These relations are tested with the JU2003, MSG05, and MID05 data in later sections.

Sonic anemometers are necessary in urban street canyons, where wind speeds are generally low and an anemometer is needed that can measure down to a few cm s^{-1}. However, no site is "representative" in such a complicated setting. Oke (2004) gives some guidelines for siting anemometers in urban areas, but it is impossible to completely avoid interferences by nearby buildings. For anemometers near street level, placement in a street canyon can predetermine the dominant local wind directions and the variation of the wind speed with the above-roof-level wind speed. For this reason, when many sonic anemometers are available, as in the field experiments studied here, they are spaced so as to cover a range of expected street orientations and intersections.

This paper makes use of sonic anemometer data from JU2003, MSG05, and MID05. The 20 DPG sonic anemometers (at z = 8 m) from JU2003 that are used in the analysis below are described by Hanna et al. (2007). There were 10 Intensive Observation Periods (IOPs) of duration eight hours, with six IOPs during the day and 4 IOPs during the night. There were no rooftop sonic anemometers during JU2003.

The MSG05 sonic anemometer data are available for six hour time periods from 8:30 am through 2:30 pm on 10 and 14 March 2005 (Hanna et al., 2006). The average building heights (H = 60 m) in the MSG area in Manhattan are about three or four times what they are in JU2003, and Manhattan is about four or five times wider. The two IOP days included seven sonic anemometers (five are used here) at street level (at z = 3 m) and two on very tall buildings. Rooftop anemometers were on the One Penn Plaza (OPP at 233 m) and Two Penn Plaza (TPP at 153 m) buildings, at a height of 5 to 10 m above the rooftop. Both IOPs were marked by similar wind speeds (about 5 m s^{-1}), directions (WNW to NNW), and temperatures (slightly below 0.0 C).

The MID05 field experiment (see Figure 1) took place in August 2005, on a larger domain centered about two km to the northeast of MSG, covering the so-called Midtown area of Manhattan. The 10 surface anemometers

were at a height of 3 m. The 5 rooftop anemometers were on the Met Life (MetL1, 247 m), OPP (233 m), McGraw-Hill (MGH1, 208 m), General Motors (GM1, 225 m), and Park Plaza (PPZ, 182 m) buildings, at a height of 6 m above the rooftop. Sonic anemometer data were analyzed from the six IOPs for 7 ½ hour periods from 5:00 am through 12:30 pm EST. Wind speeds were generally lighter than during MSG05.

2. RESULTS OF ANALYSIS OF TURBULENCE

The 10 Hz records from the sonic anemometers have been used to calculate the following variables over a 30 min averaging times for this analysis: mean wind components, mean temperature, standard deviations (s.d.'s) of wind component fluctuations (σ_u, σ_v, and σ_w), s.d. of horizontal wind fluctuations ($\sigma_h = (\sigma_u^2 + \sigma_v^2)^{1/2}$), TKE = $(\sigma_u^2 + \sigma_v^2 + \sigma_w^2)/2$, s.d. of temperature fluctuations σ_T, friction velocity u*, temperature scale T*, and Monin-Obukhov length L. The total horizontal velocity turbulent s.d., σ_h, is used because of the large turbulent intensities in urban areas.

Hanna et al. (2007) review a set of similarity relations observed in other cities and present a summary of recommendations by Britter and Hanna (2003) for turbulent variables in urban areas. Table 1 extracts some observations of dimensional and nondimensional s.d.'s and u* and T* from the calculations for MSG05 and MID05, includes the same data from JU2003, and compares the observations at the three sites with the relations suggested in the references.

The last eight rows of Table 1 present the average values of the dimensional variables. The median is given for T* and L. The turbulent speeds and u* obviously scale with wind speed, u, as expected. The temperature s.d., σ_T, is in the range from about 0.4 to 0.6 °C and the temperature scale, T*, is about 0.2 °C at the surface during the day at the three sites. The median Monin-Obukhov length, L, is negative and with relatively large magnitude, day and night, at the surface and the rooftops, suggesting persistent slightly-unstable conditions in the built-up downtown areas. For daytime conditions, and for either surface or rooftop anemometers, most of the dimensionless turbulence averages are very similar (within about 20 %) for JU2003, MSG05, and MID05.

Table 1 uses both u* and u to normalize the turbulent velocities. The average ratio u*/u is about 0.24 for the surface measurements and about 0.13 for the rooftop measurements. The surface value agrees fairly well with the postulated value of 0.28. The observed average and values of σ_u/u, σ_v/u, and σ_w/u near the surface are 0.50, 0.56, and 0.31, which are within 40 % of the postulated values of 0.45, 0.39, and 0.31, respectively. When u* is used for scaling, the observations of scaled horizontal wind speed s.d.'s (e.g., σ_u/u^*) from the three sites near the surface tend to be consistently higher, by about 50 to 80 %, than postulated by Britter and Hanna (2003). The observed TKE is about 3 times larger than the expected values.

The observed JU2003, MSG05, and MID05 temperature s.d., σ_T, divided by the scaling temperature, T*, can also be compared with published similarity relations. The average values of σ_T/T^* at JU2003, MSG05, and MID05 at the surface are about -3.24, -3.63, and -1.95, which correspond to the value postulated by the references for nearly neutral conditions, on the slightly-unstable side. These findings are consistent with the known daytime weather conditions during the field experiments. Even for the nighttime experiments in JU2003, the T* and L values indicate slightly-unstable conditions.

3. VARIATION OF TURBULENCE IN TIME AND SPACE

The analysis in Section 2 of observed 30-minute averaged urban turbulence focused on average values averaged over time or over a group of similar locations. The urban domain, more so than most other domain, is likely to show variations in time and in space due to the influence of the buildings. This effect is investigated for MID05 in this section. In general it is found that the contribution of the time and space variations to the total s.d. is less than 50 % of the average 30-min s.d. quoted in Section 2. This is encouraging, since it verifies that the conclusions in section 3 are generally valid and are not overwhelmed by site-to-site variations or time variations from one 30 min average to the next.

The variations (measured by the s.d., STD) over time and/or space are calculated in three different ways:
1) Space and time (s&t) variations are based on the 15 30 min averages during an IOP and the 12 sites (at the surface) or 5 sites (at the rooftops). Thus there is a maximum of 15x12 = 160 numbers at the surface and 15x5

= 75 numbers at the rooftops for calculating the variation. Then the STDs for the six IOPs are averaged to give the numbers in the table. 2) The space (s) variations are based on the STD over the 12 (surface) sites during each 30 min period. 3) The time (t) variations are based on the STD for each site over the 15 30-min periods during each IOP. Typically, for the surface anemometers, the magnitude of STD(s) is about 90% of the magnitude of STD (s&t) and the magnitude of STD (t) is about 70 % of the magnitude of STD (s&t). The 70 % ratio between STD (t) and STD (s&t) is valid for the rooftop anemometers, too.

The ratios of the STD of a mean variable (WS, w, and T) to the mean 30-min average turbulent s.d. of that variable are also calculated. STD(WS)/σ_h is about 0.4 or 0.5, STD(w)/ σ_w is about 0.4, and STD(T)/ σ_T is about 3.8 at the surface and 2.4 at rooftop.

4. CONCLUSIONS

Some results are given of analyses of the JU2003, MSG05, and MID05 observations of fast response winds and temperatures. These urban data are unique because the focus was on turbulence near street level (i.e., the surface) in the built-up downtown areas. The results are encouraging in the sense that similar scientific relations appear to be evident in three experiments. The following tentative conclusions have been reached: Calculations from sonic anemometer observations of wind and temperature fluctuations in downtown areas during JU2003, MSG05, and MID05 suggest that turbulence quantities such as σ_u, σ_w, σ_T, and u* are fairly robust. Nondimensional relations such as $\sigma_w/u^* = 1.5$ and $u^*/u = 0.24$ are shown to be valid for these urban data. Only small differences are seen in the results for day versus night (i.e., stability) for these urban downtown turbulence relations. Daytime heat fluxes are slightly unstable and nighttime heat fluxes are slightly unstable, as shown by the values of the Monin-Obukhov length. The variations between the surface and rooftops are investigated using the Manhattan MSG05 and MID05 data, showing that most of the turbulent speed s.d.'s at the surface are about 40 or 50 % of their values at the rooftops. The variations at MID05 in the 30-minute mean turbulence values with time (i.e., 15 30-min time periods each IOP) and with site (i.e., 12 surface sites) were calculated in order to estimate their magnitude compared to the 30 min averages of σ_u etc. It is found that the space and time variations are generally less than 50 % of the 30 min averages analyzed above.

5. ACKNOWLEDGEMENTS

This research has been sponsored by the U.S. National Science Foundation, the U.S. Department of Homeland Security, and the U.S. Defense Threat Reduction Agency. The authors appreciate the assistance provided by Michael Reynolds and Victor Cassella of Brookhaven National Laboratory, who have supplied most of the MSG05 and MID05 meteorological data. The authors also thank Drs. Jerry Allwine and Julia Flaherty, who have put together the MSG05 and MID05 data archives.

6. REFERENCES

Allwine K. J., Leach, M., Stockham, L., Shinn, J., Hosker, R., Bowers, J. and Pace, J. 2004. Overview of Joint Urban 2003 – An atmospheric dispersion study in Oklahoma City. Preprints, Symposium on Planning, Nowcasting and Forecasting in the Urban Zone. American Meteorological Society, January 11-15, 2004, Seattle, Washington.

Britter, R. E., and Hanna, S. R. 2003. Flow and Dispersion in Urban Areas. Annu. Rev. Fluid Mech. 35, 469-496.

Clarke, J. F., Ching, J. K. S., Godowitch, J.M. and Binkowski, F. S. 1987. Surface layer turbulence in an urban area. Modeling the Urban Boundary Layer. ISBN-0-933876-68-8, AMS, 45 Beacon St., Boston, MA 02108, 161-200.

Hanna, S.R., Brown, M.J., Camelli, F.E., Chan, S., Coirier, W.J., Hansen, O.R., Huber, A.H., Kim, S., and Reynolds, R.M. 2006. Detailed simulations of atmospheric flow and dispersion in urban downtown areas by Computational Fluid Dynamics (CFD) models – An application of five CFD models to Manhattan. Bull. Am. Meteorol. Soc., 87, 1713-1726.

Hanna, S.R., White, J., and Zhou, Y. 2007. Observed winds, turbulence, and dispersion in built-up downtown areas in Oklahoma City and Manhattan. to appear in Bound.-Layer Meteorol.

Oke, T. R. 2004. Initial Guidance to Obtain Representative Meteorological Observations at Urban Sites. World Meteorological Organization Instruments and Observing Methods Report No. 81 (WMO/TD No. 1250), 47 pages.

Rotach, M. W. 1995. Profiles of turbulence statistics in and above an urban street canyon. Atmos. Environ. 29**,** 1473-1486

Roth, M. 2000. Review of atmospheric turbulence over cities. Quart. J. Roy. Meteorol. Soc. 126, 941-990.

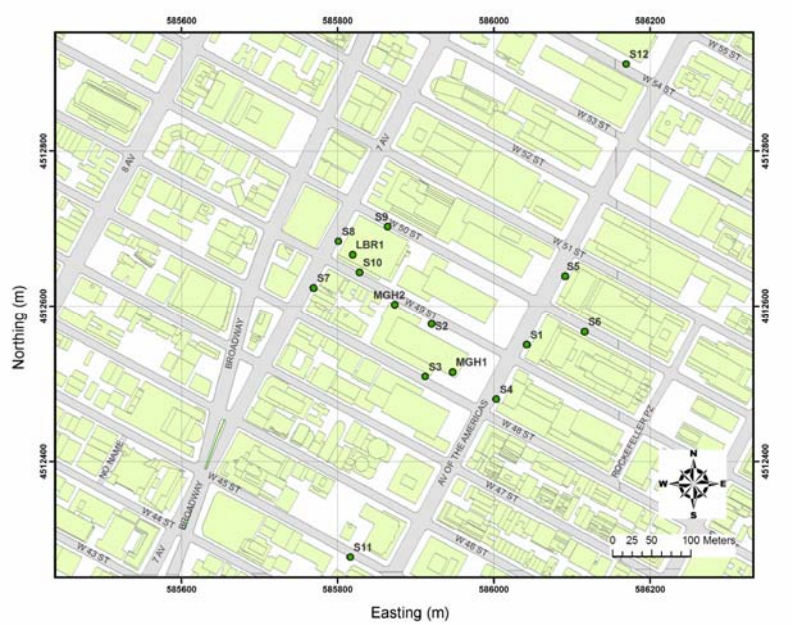

Figure 1. Central portion of the MID05 area, showing locations of sonic anemometers. The letter S refers to "surface". The figure was prepared by Julia Flaherty.

Table 1. Comparison of JU2003, MSG05 and MID05 Mean Turbulence Observations with Summary Results from the Literature. "Sfc" is at height 3 to 8 m. "Roof" (or rf) is at rooftop of tall buildings (typical heights of 150 to 250 m). All Measurements are Local. If no "day-night" or "sfc-roof" breakdown is given, the difference is less than 2 or 3 %.

Turb Quantity	***Recs from Literature***	***JU2003 Obs (all at surface)***	***MSG05 Obs (all during daytime)***	***MID05 Obs (all during daytime)***	***Avg over Three Field Exps***
σ_u/u^*	1.6 sfc, 2.4 roof	2.36	2.00 sfc, 3.90 rf	3.12 sfc, 3.44 rf	2.49 sfc, 3.69 rf
σ_u/u	0.45	0.50	0.44	0.55 sfc, 0.47 rf	0.50 sfc, 0.45 rf
σ_v/u^*	1.4 sfc, 1.9 roof	2.36	1.71 sfc, 3.78 rf	3.18 sfc, 3.49 rf	2.42 sfc, 3.65 rf
σ_v/u	0.39	0.50	0.60 sfc, 0.43 rf	0.57 sfc, 0.50 rf	0.56 sfc, 0.44 rf
σ_h/u^*	2.1 sfc, 3.1 roof	3.63	3.47 sfc, 5.58 rf	4.50 sfc, 4.96 rf	3.87 sfc, 5.27 rf
σ_w/u^*	1.1 sfc, 1.3 roof	1.56	1.36 sfc, 1.81 rf	1.80 sfc, 1.60 rf	1.57 sfc, 1.70 rf
σ_w/u	0.31	0.33	0.29 sfc, 0.20 rf	0.32 sfc, 0.23 rf	0.31 sfc, 0.22 rf
TKE/u^{*2}	2.87 sfc, 5.53 roof	6.9	7.01 sfc, 16.8 rf	10.1 sfc, 11.7 rf	8.01 sfc, 14.3 rf
σ_T/T^*	-3	-2.28 day, -4.68 night	-3.63 sfc, -6.63 roof	-1.95 sfc, -2.12 roof	Day -2.62 sfc, -4.38 rf
u^*/u	0.28 sfc downtown	0.25	0.27 sfc, 0.11 rf	0.20 sfc, 0.16 rf	0.24 sfc, 0.13 rf
σ_h (m/s)		1.61	1.88	0.94 sfc, 2.09 rf	
σ_w (m/s)		0.69	0.74 sfc, 1.17 rf	0.37 sfc, 0.68 rf	
TKE (m^2/s^2)		2.32	2.12 sfc, 7.11 rf	0.53 sfc, 2.04 rf	
σ_T (°C)		0.41 day, 0.17 night	0.61 sfc, 0.89 roof	0.53 sfc, 0.66 roof	
u (m/s)		2.11	2.53 sfc, 5.74 rf	1.18 sfc, 2.99 rf	
u^* (m/s)		0.44	0.55 sfc, 0.65 rf	0.24 sfc, 0.49 rf	
T^* (°C)		-0.18 day, -0.04 night	-0.17 sfc, -0.26 roof	-0.25 sfc, -0.49 roof	
L (m) median		-270 day, -900 night	-130 sfc, -100 roof	-28 sfc, -147 roof	

Proceedings of the 6th International Conference on Urban Air Quality
Limassol, Cyprus, 27-29 March 2007

QUASI-STEADY STATE EQUILIBRIUM BOUNDARY LAYER HEIGHT DETERMINATION IN URBAN CONDITIONS

Amela Jeričević
Croatian Meteorological and Hydrological Service, Grič 3, 10000 Zagreb, Croatia
jericevic@cirus.dhz.hr

ABSTRACT

The evolution of the urban boundary layer height (H) in stable conditions is often highly nonstationary and quasi-steady state equilibrium height is very slowly approached from the initial state after sunset. Nevertheless, diagnostic methods strictly valid for stationary conditions have been widely used in practical applications and prognostic equations are rarely validated. Here, diagnostic bulk Richardson method (Ri_B) and linear relaxation prognostic equation are applied on the radio soundings at urban site and the corresponding numerical weather prediction data (NWP) to determine H in stable conditions. The underestimation and hour to hour unrealistic variation of the modelled H in diagnostic approach is shown for night-time neutral and stable situations. Prognostic approach gives smoother transition to equilibrium state. On the other hand, in very stable conditions diagnostic and prognostic approach are similar due to stationary conditions.

1. INTRODUCTION

Stable boundary layer height (H), either measured or determined from an atmospheric model, is a very important and complex parameter used in many meteorological applications. Even though the models provide numerical values of H with high resolution in space and time, they still represent a simplification of reality especially in urban areas Representation of the boundary layer structure in all its complexity and variability depends on the specific model characteristics and applied parameterisations. Therefore a continuous comparative assessment of H calculated from various data sources and with different methods is needed.

The evolution of urban H is highly non-stationary, especially during the first few hours after sunset. Even later during the night an approach to quasi-steady state equilibrium height (He) can be very slow. Basically, we can distinguish two approaches for the determination of H: diagnostic and prognostic. The prognostic equation that describes the development of H toward He ought to be better than a diagnostic relationship in modelling evolution of the H under stable but also evolving conditions. According to Seibert et al., (2000), the prognostic equations have rarely been tested systematically; only single case studies are typically reported (e.g., Hanna, 1969; Arya, 1981; Koračin and Berkowicz, 1988). In Zilitinkevich et al. (2002) diagnostic and prognostic equations for the depth of stably stratified Ekman boundary layer are validated against measurements. Moreover, H from NWP models in urban stable conditions needs to be analyzed through diagnostic and prognostic equations. Here ALADIN (Aire Limitee Adaptation Dynamique development InterNational) (Geleyn et al. 1992), a spectral hydrostatic limited area NWP model for short-range forecasts, is used.

One goal of this study is to test two different methods for determination of H: a prognostic equation of a linear relaxation type, and widely used diagnostic bulk Richardson number, Ri_B, method (Mahrt, 1981; Troen and Mahrt, 1986; Holtslag et al. 1990; Sørensen et al. 1996; Jeričević and Grisogono, 2006). These methods are applied on radio sounding and NWP data in an urban area where stationary conditions are very rare. Urban areas are characterized with enhanced and more continuous turbulence while surface cooling is decreased by urban heat island effects (e.g., Arya, 1999).

2. METHODS AND DATA USED FOR DETERMINATION OF H IN SBL CONDITIONS

2.1. PROGNOSTIC AND DIAGNOSTIC METHODS

Prognostic relations for H in SBLs are usually characterized by a linear relaxation equation (Nieuwstadt and Tennekes, 1981; Arya, 1981; Seibert et al., 2000; Zilitinkevich et al., 2002a):

$$\frac{dH}{dt} = \frac{(He - H)}{\tau}, \qquad (1)$$

where the rate of change of H toward its equilibrium He is governed by the time scale τ, being here proportional to $1/f$, where f is a Coriolis parameter. A prognostic equation proposed in literature (Khakimov, 1976) is applied:

$$\frac{dH}{dt} = 1.5 f (He - H) . \quad (2)$$

Integration of Eq. (2) yields:

$$H(t) = He - (He - H(1))\, e^{-1.5 \cdot ft} , \quad (3)$$

where H (1) is the value of H at the onset of the SBL development, i.e., after sunset. Initial values H (1) used in Eq. (3) are extrapolated from radio soundings and from the model at 12 UTC.

In practical applications He is determined from diagnostic equations. In this study He was calculated by the Ri_B method:

$$He = Ri_B \frac{\overline{\theta}}{g} \frac{U^2(h)}{\theta(h) - \theta_S} . \quad (4)$$

This method is based on the assumption that continuous turbulence vanishes beyond Ri_{Bc}, some previously defined critical value of Ri_B. The height at which Ri_B reaches Ri_{Bc} is considered as H. The critical value used here is Ri_{Bc}=1.5 and applied on urban radio soundings data and in the NWP model. This Ri_{Bc} value is used because it is shown that it is the most appropriate for urban SBL conditions (Jeričević and Grisogono, 2006).

2.2. DATA

Nocturnal 15 days seasonal periods are selected from radio soundings performed operationally at 12 and 00 UTC in Zagreb, Croatia. Analysed periods are 25 January – 8 February 2002, 7 – 21 May 2002, 7 – 21 August 2002 and 7 – 21 October 2002. Varieties of nocturnal situations were encountered, ranging from neutral or weakly stable conditions with continuous turbulence to very SBL (Mahrt, 1981) conditions with week winds and intermitted turbulence.

The measuring site can be considered as urban or suburban, its detailed description is in Jeričević and Grisogono (2006). Radio sounding measurements in Zagreb are performed since 1956, and at first measuring area was basically rural with the town centre to W, and forest to NE. Due to the city growth during the last 50 years, nowadays this area consists of factories, buildings and traffic roads. The estimated surface roughness, according to Wind Atlas Analysis and Application Program WA^{S}P-User's Guide (Mortensen et al., 1993), for this area of a few square kilometres, is in the interval 0.8 m $\leq z_0 \leq$ 1 m.

3. RESULTS AND DISCUSSION

3.1. RADIO SOUNDINGS AND NWP MODEL

The diagnostic Ri_B and prognostic methods are applied on the NWP model output to calculate H. In Fig. 1. the night time evolution of hourly $H\__{ALADIN}$ determined by the diagnostic and prognostic methods are represented for periods of approximately 15 days in different seasons. In the same figure hourly values of H_soundings are also plotted. The analysed winter period was characterized with very stable night time conditions with weak winds and strong positive temperature gradients. In those conditions H was very low and had stationary character. Since initial and equilibrium H_soundings was quite similar, there was no significant growth from the initial toward equilibrium values and the conditions were nearly stationary. Due to the predicted slowly-varying conditions in the NWP model, the initial and equilibrium values were also similar, i.e., $H\__{ALADIN}(1) \approx He\__{ALADIN}$. Therefore, in the very SBL ,according to Eq. (3), the modelled hourly H values had approximately constant values. Both approaches, diagnostic and prognostic, applied on the NWP data gave almost same results e.g., 25 and 29 January 2002, but it should be noted that for these days H_soundings were much higher since the observed conditions at 00 UTC were more near -neutral. Also both initial values H(1), modelled and measured, were in good agreement but He differed significantly, $\Delta He \approx 600$ m. In the spring period the model predicted stable night time conditions and H was slowly converging toward He. Initial values H(1) determined from the model by the diagnostic and prognostic approach were relatively high, around 1000 m, while He was less than 100 m. In this spring period, and also for 9-14 August 2002, agreement with the soundings also strongly depended on H(1) and He; therefore, differences mostly occurred due to differences in determined He.

These differences may occur due to the model or soundings errors. Radio soundings possible limitations occur because they represent snapshots of reality and therefore subject to random errors due to

fluctuations caused by eddies and also if the time response of the radiosonde instruments is too long, some sharp changes in the profiles can be smoothed artificially. The NWP model also has its own limitations of another nature than soundings: errors in prediction, limitations according to parameterisation and resolution used etc. Note that the diagnostic approach underestimated H, especially in spring and summer periods, and more stationary night time development was recorded in all periods. Further, significant and sharp oscillations between two model hours in H_{ALADIN} determined by diagnostic approach are shown e.g. 10 and 12 August, or 10 and 11 October in Fig. 1. This hour to hour oscillations in H may be very inconvenient for dispersion modelling purposes.

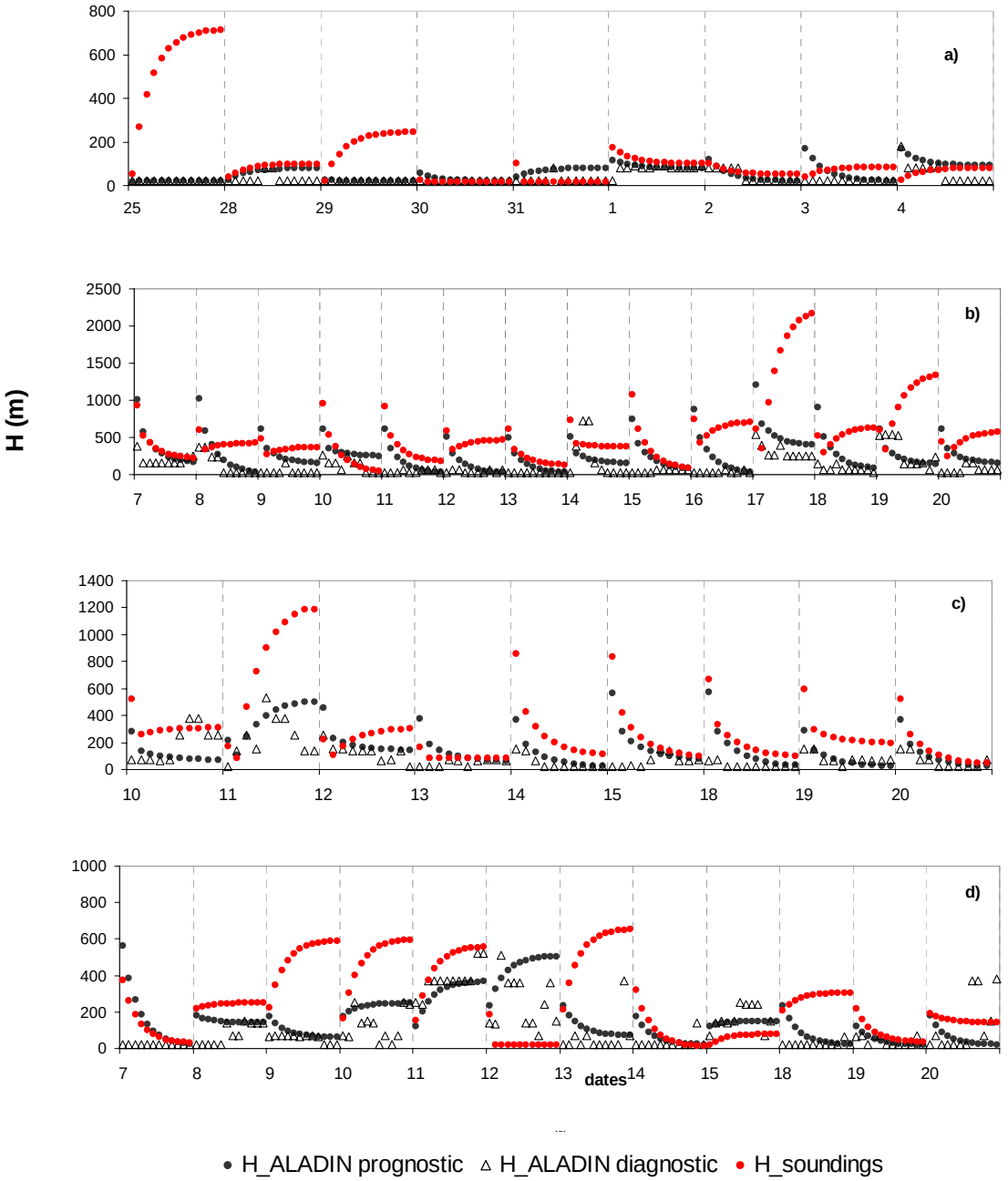

Fig. 1. Night time evolution of hourly diagnostic H_{ALADIN}, calculated with the Ri_B method and H_{ALADIN} calculated with linear prognostic equation of relaxation type Eq. (4) from ALADIN model and H_soundings determined by (3) from soundings for a) 25 January-8 February 2002, b) 7-21 May 2002, c) 7-21 August 2002 and d) 7-21 October 2002 in Zagreb, Croatia

4. CONCLUSIONS

The analysis presented, based on significant data set (more than 200 hourly values) of hourly H calculated from radio sounding measurements and NWP data, showed that the prognostic approach can be more convenient for the H determination in urban night time conditions. Although the diagnostic approach has been widely used for calculation of H from NWP models, a relatively simple prognostic equation is easy to use as an alternative in complex mesoscale NWP models. The diagnostic approach typically showed stationary conditions and an underestimation of H was often detected. Based on theory and measurements it is reasonable to expect higher values of H in urban stable conditions. Relatively high night time urban H determined from the model and measurements is not unusual. Differences between rural and urban H can be up to 40% (Arya, 1999), or 45%, that is $\Delta H_{UR} \approx 700m$ (Angevine at al., 1999) especially in the SBL. Inappropriateness of diagnostic approaches in night time stable conditions was also showed in other studies of SBL conditions where diagnostic methods applied on NWP data underestimated H even in rural areas (Seibert et al., 2000; Baklanov, 2002; Zilitinkevich and Baklanov, 2002). Since urban areas are characterized with horizontal unhomogeneity and temporal non-stationarity, the use of a diagnostic equation may be inappropriate for H. The main advantage of the prognostic method is a smooth attainment of the equilibrium state and better chance to avoid an underestimation of H.

5. ACKNOWLEDGEMENTS

I am grateful to Branko Grisogono on important comments and advise concerning the final form of this paper. This work is partly supported by the Croatian Ministry of Science, Education and Sport, under the projects number 0004001.

6. REFERENCES

Angevine, W.M., White, A.B., Senff, C.J., Trainer, M., Banta, R.M., Ayoub, M.A., 1999. Urban-rural contrasts in mixing heights and cloudiness over Nashville in 1999. J. Geophys. Res. 108, 10.1029/2001JD001061, AAC 3-1 - AAC 3-10, 2003.

Arya, S. P., 1981. Parameterizing the height of the stable atmospheric boundary layer, J. Appl. Meteorol. 20, 1192-1202.

Arya, S. P., 1999. Air pollution meteorology and dispersion. 1st edn. Oxford University Press, New York, 310 pp.

Baklanov, A., 2002. Parameterisation of SBL height in atmospheric pollution models. In: Air pollution Modelling and its Application XV. Borrego, C. and Schayes, eds., Kluwer Academic / Plenum Publishers, New York, pp. 303-310.

Geleyn, J. F., Banciu, D., Bubnova, R., Ihasz, I., Ivanovici, V., Le Moigne, P., Radnoti, G., 1992. The international project ALADIN: summary of events October 1992 - October 1993. LAM Newsletter 23.

Hanna, S. R., 1969. The thickness of the planetary boundary layer, Atmos. Environ. 3, 519-536.

Holtslag, A. A. M., De Bruin E. I. F., Pan H. - L., 1990. A high resolution air mass transformation model for short range weather forecasting. Mon. Wea. Rev. 118, 1561-1575.

Jeričević, A., Grisogono B., 2006. The critical bulk Richardson number in urban areas: verification and application in a numerical weather prediction model. Tellus A 58, 19-27.

Khakimov, I. R., 1976. The wind profile of the neutrally stratified atmosphere boundary layer, Izv. Acad. Sci., U.S.S.R., Atmospheric and Oceanic Phys. 12, 628-630.

Koračin, D., Berkowicz R., 1988. Nocturnal boundary layer height: observation by acoustic sounders and prediction in terms of surface layer parameters. Boundary-Layer Meteorol. 43, 65-83.

Louis, J.F. 1979. A parametric model of vertical eddy fluxes in the atmosphere, *Boundary-Layer Meteorol.* **17,** 102-187**.**

Mahrt, L., 1981. Modelling the depth of the stable boundary layer. Boundary-Layer Meteorol. 21, 3-19.

Mortensen, N.G., Landberg, L., Troen, L., Petersen, E.L., 1993. Wind atlas analysis and application program –WasP. Vol. 2: User's guide. Risø National Laboratory, Roskilde, Risø-I-666(v.2)(EN)

Seibert, P., Beyrich, F., Gryning, S.- E., Joffre, S., Rasmussen, A., Tercier, Ph., 2000. Review and interscomparison of operational methods for the determination of the mixing height. Atmos. Environ. 34, 1001-1027.

Sørensen, J. H., Rasmussen, A., Svensmark, H., 1996. Forecast of atmospheric boundary-layer height for ETEX real-time dispersion modelling. Phys. Chem. Earth. 21, 435-439.

Troen, IB., Mahrt, L., 1986. A simple model of the atmospheric boundary layer; sensitivity to surface evaporation. Boundary-Layer Meteorol. 37, 129-148.

Zilitinkevich, S., Baklanov, A., 2002. Calculation of the height of the stable boundary layer in practical applications. Boundary-Layer Meteorol. 105, 389-409.

Zilitinkevich, S., Baklanov, A., Rost, J., Smedman, A.- S., Lykosov, V., Calanca P., 2002. Diagnostic and prognostic equations for the depth of the stably stratified Ekman boundary layer. Quart. J. Roy. Meteorol. Soc. 128, 25-46.

Proceedings of the 6th International Conference on Urban Air Quality
Limassol, Cyprus, 27-29 March 2007

RELATIONSHIPS BETWEEN AIR POLLUTION AND METEOROLOGY IN NEWCASTLE, AUSTRALIA

Howard Bridgman and James O'Connor
School of Environmental and Life Sciences
University of Newcastle NSW 2308 Australia

ABSTRACT

We calculated relationships between daily synoptic category, temperature, humidity, wind speed, local pressure, ozone, nitrogen oxides and PM10 for 2001-2002 for Newcastle, located on the SE coast of Australia, using Factor Analysis. Daily synoptic maps were classified into 10 categories based on the location of the centre of the relevant high or low pressure system compared to Newcastle. Despite pollution concentrations remaining below Australian national standards, several significant relationships were found. For example for category 10, high pressure to the east and a cold front approaching from the west, significant relationships occurred between temperature, lower wind speeds, and high PM10 (Factor 1); pressure, nitrogen oxides, low wind speeds and low ozone concentrations (Factor 2); and high humidity with low PM10 (Factor 3). These results were not unusual, but the relationship with synoptic category allows the possibility of prediction of periods of higher air pollution concentrations, which improves management planning.

1. INTRODUCTION

The city of Newcastle on the east coast of Australia (33^{o}S 152^{o}E) has had a historical problem with high levels of particulate matter, sulfur dioxide and nitrogen oxides due to heavy industrial emissions, that has create a major interest in air pollution management (Bridgman *et al.* 1992; Bridgman and Graham 2005). The closure of some of these industries in the 1990s, especially the major source of pollutants, BHP Rod and Bar Steel Works, has created major improvements in air quality levels (especially for SO_2 and PM10), but concerns about fine particulates (PM2.5) and increasing photochemical pollution levels (ozone O_3) remain.

As well as the amount and type of pollutants emitted by human activities, poorer air quality can be influenced by local and synoptic meteorological conditions. For example, investigations in Australia by Hess *et al.* (2004) and others established high urban summer O_3 concentrations are enhanced by stagnant synoptic high pressure systems, low level local inversions, and sea breeze recirculation. Such results are not unusual and have been found for larger cities around the world, such as Athens (Statheropolis *et al.* 1998), Birmingham UK (McGregor and Bamzelis 1995), and other locations (Comrie 1996 and others). An understanding of the role of meteorology in urban air pollution dispersion can assist in identifying pollution episode periods, in the evaluation of local pollution transport problems, to establish a basis for local air pollution modeling, and to assist air pollution management decisions.

The change in pollution concentrations with industry closure in Newcastle, and the availability of a good quality meteorological and air pollution data set provided the opportunity to assess air pollution and meteorological relationships for the city for the period 2001-2002. While the concept is not new, its application to a small urban area (147,000 people) in a coastal situation, where current pollution levels remain below national health standards, is unusual.

2. METHODOLOGY

Meteorological and air pollution data were obtained from the New South Wales Department of Environment and Conservation (NSWDEC) monitoring site in Newcastle for 2001 and 2002. Daily average values of NO_x (representing NO_2), PM10 and O_3 were compiled, but the SO_2 data set was too incomplete to be used. No more than 20 days of data were missing for the other three pollutants. We also included the NSWDEC daily Regional Pollution Index for Newcastle, which is calculated from particulate and photochemical measurements. Meteorological data included average, maximum, and minimum temperature, average relative humidity, and average wind speed. Daily mean sea level pressure was determined from the nearest Bureau of Meteorology (BOM) site, at Williamtown 12 km to the north.

Synoptic meteorological categories were determined from the 1000 EST (0000 UTC) surface weather charts downloaded from the BOM web site (www.bom.gov.au) archives. Using Newcastle as a central point, each chart (east coast of Australia) was quartered. The synoptic weather for each day was classified according to the quadrant where the dominant pressure system was located. The sea level pressure (hpa) for Newcastle was then determined, and divided into 4 categories (<1006, strong low; 1006-1013, weak low; 1014-1020, weak high; >1020 strong high). 20 synoptic categories (SC) were then defined according to quadrant and pressure categories. Half these categories occurred on very few charts, and therefore were combined with the nearest representative category. Table 1 presents the final categories used in this project. In order of

frequency of occurrence, the dominant SCs (>80 days) were 12, 11, 16, 15, and 14, with 10 occurring on about 65 days, the other four occurring on 40 days or less each.

Table 1. Synoptic categories used in this analysis

Category	Dominant Season*	Description
3	Winter	Weak high, NW quadrant
4	Winter	Strong high, NW quadrant
10	Summer	Weak low, SW quadrant
11	Summer	Weak high, SW quadrant
12	Winter	Strong high, SW quadrant
14	Summer	Weak low, SE quadrant
15	Summer	Weak high, SE quadrant
16	Winter	Strong high, SE quadrant
18	Summer	Weak transitional
19	Both	Strong transitional

*Based on frequency of category occurrence during the year.

The daily data set was divided into the synoptic categories listed in Table 1, and analysed statistically using Factor Analysis (FA). FA has been successfully used in this type of analysis in several different studies (*i.e* Stone 1989; Bridgman 1992; McGregor and Bamzelis 1995). Its benefits are that it allows correlations in large data sets to be calculated, creating a series of matrices and pre-numbered factors (Gorsuch 1983). A standard Statistical Analysis System (SAS) package was used for the calculations, incorporating orthogonal rotation to assist in the lineup of the factors. Experimentation indicated that three factors were the most appropriate for each synoptic category. Although some questions about the applicability of FA to these kinds of data sets have been raised (see Bridgman 1992), the results can be considered at least representative.

3. RESULTS AND DISCUSSION

Table 2 presents the range of conditions for each meteorological and air pollution parameter included in the study (Tmax is used to represent the temperature categories). The meteorological results are typical for a sub-tropical location that is can affected by global westerlies in the winter. 2001 and 2002 were overall drier on average, according to BOM summaries (www.bom.gov.au). All air pollution results were within national health standards (Bridgman and Graham 2005).

Table 2. Summaries of parameters used in the study, 2001-2002, daily values

Parameter	Maximum	Minimum	Comments
Sea Level Pressure (MSLP, hPa)	>1030	<1006	Overall slightly higher in summer
Wind Speed (ms^{-1})	7.5	0.5	Higher in summer
Maximum Temp (Tmax, ^oC)	38	12	Higher in summer
Ozone (O_3, pphm)*	4.5	0.3	Higher in summer
Nitrogen Oxides (NO_x, pphm)$^+$	12.0	0.1	Higher in winter
Particulates (PM10, µg m^{-3})$^\#$	100	0.05	No seasonal trend

* National health standard 8 pphm for 4 hours; + National health standard 3 pphm for 1 year;
#National health standard 50 µg m^{-3} for 24 hours, 5 exceedences per year allowed

Table 3. Factor analysis results for two summer-dominant synoptic categories (see Table 1)

	Synoptic Class 10			Synoptic Class 14		
Parameter	Factor 1	Factor 2	Factor 3	Factor 1	Factor 2	Factor 3
Tmax	0.92			0.90		
Tmin	0.82		*0.46*	0.92		
Tave	0.96			0.96		
RH			0.84		-0.70	
MSLP		0.50			-0.59	
Wind Speed	*-0.48*	-0.71				-0.71
O3		-0.65	-0.57		0.79	
PM10	0.69			0.81		
NOx		0.88				0.79
RPI	0.63		-0.63	0.65	0.64	
VE*	3.70	2.10	1.78	4.12	1.98	1.34

*Variance Explained

Table 3 presents FA results for two of the SCs that occur dominantly in summer. Only factors 0.5 or greater are presented as significant, following procedures by Bridgman (1992). Correlations between 0.4 and 0.5 are shown in italics to assist the discussion.

In both cases, temperature dominates Factor 1, and there is a clear relationship with higher PM10. RPI also correlates strongly, suggesting that particulates dominate the RPI calculation in this Factor. There is a weak link with lower wind speed in SC10 but not in SC14. Factor 1 clearly dominates the variance explained, especially for SC14.

Factor 2 differs between SC10 and 14. Higher pressure and NO_x concentrations relate to lower wind speed and O_3 in SC10. Since NO_x dominates the chemistry of photochemical pollution production (Turco 1997), and NO_2 reduces when O_3 increases, an opposite relationship of these two gases is logical. For SC14, O_3 and RPI are linked, showing O_3 is the dominant RPI pollutant, and there is a correlation with lower RH and pressure. This result is similar to Factor 3 in SC10, and may reflect the greater importance of weak low pressure in defining this SC.

Factor 3 for SC10 shows the RPI and O_3 to be significantly lower under higher RH. There is a weak link with minimum temperatures. Factor 3 for SC14 is more similar to Factor 2 in SC10, where higher NO_x occurs under lower wind speeds.

Overall, these two SCs show broadly similar FA results, but the relationship between higher NO_x and lower wind speed (and O_3) is more important under SC10 conditions. The other summer-dominated SCs, 11, 15, and 18, differ only in detail. In SC11, the PM10 and RPI correlation is in Factor 3, not Factor 1. In SC15, O_3, PM10 and RPI are strongly related in Factor 2, with similar results in SC18. In both these SCs, the opposite correlation between O_3 and wind speed, and NO_x, appears in Factor 3.

Table 4. Factor analysis results for two winter-dominant synoptic categories (see Table 1)

	Synoptic Class 3			Synoptic Class 12		
Parameter	Factor 1	Factor 2	Factor 3	Factor 1	Factor 2	Factor 3
Tmax	0.87			0.94		
Tmin	*0.49*	-0.57	0.56	0.89		
Tave	0.78		*0.49*	0.96		
RH			0.80		-0.74	
MSLP			-0.75		-0.61	
Wind Speed		-0.85			0.73	
O3	0.71	*-0.42*			0.81	
PM10		0.91			*-0.45*	0.73
NOx		0.88			-0.61	*0.49*
RPI	0.90					0.87
VE*	3.06	3.02	2.13	2.89	2.85	1.81

*Variance Explained

Table 4 presents FA results for two winter-dominated SCs. SC3 and SC4 have very similar results (both are high pressure in the NW quadrant, but different strengths). Factor 1 and Factor 2 are almost the same in terms of variance explained. Factor 1 shows strong positive correlations between temperature, O_3 and RPI, despite the wintertime situation where photochemical reactions are minimal. Factor 2 show the classical relationship between low temperature, low wind speeds, and higher PM10 and NOx, shown in many other studies (*i.e.* McGregor and Bamzelis 1995). Factor 3 shows only a relationship between meteorological parameters, although for SC4, PM10 and NO_x are included here, perhaps reflecting the stronger high pressure.

SCs 12 and 16 also have similar results. Table 1 shows both have strong high pressure systems to the east of Newcastle. Once again the variance explained between the first two factors is almost the same. Temperature by itself dominates Factor 1, but Factor 2 is more complicated. Here, lower humidity, pressure, and NO_x (weakly PM10) are correlated with higher wintertime O_3 and wind speed. The correlation with pressure is not significant in SC16. Factor 3 shows that the RPI is controlled by PM10, with also a weaker correlation to NO_x, and no significant correlation to any meteorological factor.

In comparison with SCs 3 and 4, the Factor 1 correlation between temperature, O_3 and RPI is missing in SC12 and 16; the meteorological influences are different in Factor 2; and Factor 3 contains pollutants but no meteorological parameters.

SC19 is a transitional category where there is no clear domination of any particular pressure system. FA results are a mix, with Factor 1 dominated by temperature, Factor 2 by a strong correlation between PM10, O_3 and RPI, and Factor 3 by significant positive correlations between RH, pressure, and NO_x and negative correlations with O_3 and wind speed. The variance explained for Factor 1 is 3.18, and for Factors 2 and 3, 2.36.

4. CONCLUSIONS

The purpose of this paper is to present an evaluation of the relationships between daily air pollution and meteorology in the small city of Newcastle on the SE coast of Australia, using Factor Analysis. The results are mixed, partially because pollution concentrations tend to be low, and partially because the classification of the synoptic categories can be considered somewhat subjective. Using the results from Tables 1, 3 and 4, and the incorporation of the other results, the following general conclusions can be drawn.

1. Under high pressure dominant to the NW of Newcastle in winter, there are strong positive correlations between temperature, O_3 and RPI. Of equal importance is the relationship between higher PM10 and NO_x, and low wind speeds and minimum temperatures.
2. Under strong high pressure located south of Newcastle in winter, the most important relationships are positive wind speed correlated with higher O_3, occurring when humidity, pressure and NO_x are low; and between PM10 and RPI.
3. Under weak high or low pressure located to the SW of Newcastle in summer, positive correlations between temperature PM10 and RPI dominate, and higher NO_x occurs when O_3 and wind speeds are low.
4. Under weak high or low pressure located to the SE of Newcastle in summer, the relationship are similar to 3 above, but a significant correlation between O_3 and RPI becomes more important.

These results provide some representative guidelines toward preliminary relationship between air pollution and meteorology for a city with a clean atmosphere. More details and better accuracy will appear with a longer data set, and a more accurate synoptic classification methodology.

5. ACKNOWLEDGEMENTS

The paper is based on a Master of Environmental Studies project completed by James O'Connor.

6. REFERENCES

Bridgman, H.A., 1992. Evaluating rainwater contamination and sources in Southeast Australia using factor analysis. Atmos.Environ. 26A, 2410-2412.

Bridgman, H. and Graham, L., 2005. Air pollution and meteorology in small city: a case study of Newcastle, NSW, Australia, http://meteo.bg/EUROSAP/50/paper1.html.

Bridgman, H.A., Manins, P., and Whitelock, B., 1992. An Assessment of the Cumulative Emissions of Air Pollution from Kooragang Island and the Inner Suburbs of Newcastle. Report to the NSW Department of State Development, The University of Newcastle Research Associates, 162 pp.

Comrie, A.C. 1996. An all-season synoptic climatology of air pollution in the US – Mexico border region. Prof. Geog. 48, 237-251.

Gorsuch, R.L., 1983. Factor Analysis, 2nd ed. L. Erlbaun Assoc., Hillsdale, NJ, USA.

Hess, G., Tory, K., Cope, M., Lee, S., Puri, K., Manins, P., Younf, M., 2004. The Australian air quality forecasting system. Part II: case study of a Sydney 7-day photochemical smog event. J. Appl. Meteor. 43, 663-679.

McGregor, G and Bamzelis, D., 1995. Synoptic typing and its application the investigation of weather air pollution relationships, Birmingham, United Kingdom. Theor. Appl. Climatol. 51, 223-236.

Statheropoulis, M., Vassiliadis, N., and Pappa, A., 1998. Principle componenet and cnaocal correlation analysis for examining air pollution and meteorological data. Atmos. Environ. 32, 1087-1095.

Stone, R.C., 1989. Weather types at Brisbane, Queensland: and example of the use of principle components and cluster analysis. Intl J of Climatol. 9, 3-32.

Turco, R., 1997. Earth Under Siege: From Air Pollution to Global Change, Oxford University Press, New York.

Proceedings of the 6th International Conference on Urban Air Quality
Limassol, Cyprus, 27-29 March 2007

AN INTERCOMPARISION OF DIAGNOSTIC URBAN WIND FLOW MODELS BASED ON THE RÖCKLE METHODOLOGY USING THE JOINT URBAN 2003 FIELD DATA

Steven Hanna[1], John White[2], John Hannan[3], Ronald Kolbe[4], Christopher Kiley[4], Michael Brown[5], Thomas Harris[6], Yansen Wang[7], Rick Fry[3], James Bowers[2], Dennis Garvey[7], Chatt Williamson[7], and Jacques Moussifir[8]

[1] Hanna Consultants, Kennebunkport, ME
[2]US Army Test and Evaluation Command, Dugway Proving Ground, UT
[3] US Defense Threat Reduction Agency, Ft Belvoir, VA
[4] Northrop Grumman IT, Lorton, VA
[5] Los Alamos National Laboratory, Los Alamos, NM
[6] Science Applications International Corporation
[7] US Army Research Laboratory, Adelphia, MD
[8] ARIA Technologies, Paris, France

ABSTRACT

Atmospheric Transport and Dispersion (AT&D) models used for early warning and civil response require the ability to quickly and accurately calculate downwind hazards resulting from atmospheric releases of hazardous materials. This balance between accuracy and speed is even more challenging in urban environments where building effects complicate the flow field by generating turbulent features such as wake vortices and upwind displacement zones. In an attempt to strike a balance between model speed and fidelity, several groups have developed diagnostic wind flow models for urban areas using the Röckle approach, which initializes the system by parameterizing simple vortex structures behind and around buildings. The three-dimensional wind flow is then solved using mass-consistency constraints. This paper describes the initial inter-comparison of three particular Röckle-based urban wind flow models developed by the U.S. Los Alamos National Laboratory (LANL), Science Applications International Corporation (SAIC) – ARIA, and the U.S Army Research Laboratory (ARL). The study utilizes wind and chemical tracer data collected during the Joint Urban 2003 (JU2003) field study in Oklahoma City, OK. Two Intensive Observation Periods (IOPs), are simulated with common meteorological inputs and model configurations (e.g., geographic domains, urban topography specifications and grid systems.) The model-derived wind fields are then used as input to AT&D models to simulate sulfur hexafluoride (SF_6) releases during the two IOPs. The model-derived wind and SF_6 concentration fields are analyzed and compared. Future work will involve a more thorough, quantitative analysis.

1. INTRODUCTION

Many atmospheric transport and dispersion (AT&D) models have been developed to predict downwind hazards associated with the release of hazardous materials. Incidents of serious concern include accidental releases of toxic industrial chemicals from industrial facilities or transport vehicles, radiological releases from power plants, and intentional terrorist-related releases in population centers. In order for AT&D models to be effective for early warning and civil response in the event of such incidents, they require accurate and timely meteorological data. The local wind fields, in particular, must to be faithfully depicted in order for AT&D models to provide accurate concentration and/or dosage predictions. This challenge becomes more difficult in urban environments where building effects complicate the flow field by generating features such as recirculating wakes and street canyon vortices (see Fig. 1 for an example of a street canyon vortex).

Three-dimensional wind fields that account for urban effects can be constructed through a variety of methods ranging from application of simple urban canopy parameterizations to the implementation of sophisticated full physics computational fluid dynamics (CFD) models. As the complexity of the application increases (e.g., CFD flow solutions), so does the setup time and the computational burden. In an attempt to strike a balance between model speed and fidelity, several groups have developed diagnostic wind flow models for urban areas based on the so-called Röckle [1990] approach, which initializes the system by parameterizing the geometric shapes of recirculating wakes and their flow patterns behind, over, and around buildings. Parameterizations of street canyon vortices are also given, using variables listed in Fig. 1. Following Kaplan and Dinar [1996], who were the first to implement this method in an operational urban wind flow and dispersion model, several groups have modified the basic model and coupled it with mass consistency algorithms to generate detailed flow fields within the urban environment within a matter of minutes. Dispersion models (usually Lagrangian particle models) can then be utilized to quickly predict concentrations of hazardous substances.

The Röckle approach was designed to estimate realistic urban wind flow features given an upwind ambient wind profile input and a simple parameterization of wake features in the vicinity of buildings such as recirculating wakes, street canyon vortices (Fig. 1), and displacement zones on the tops of buildings. The approach requires only the upwind wind profile and detailed representation of the underlying building three-dimensional geometry (with resolution of about 1 to 5 m).

In this paper, simulations from three such models are compared using data from the Joint Urban 2003 (JU2003) field study in Oklahoma City, OK, USA. JU2003 measurements were taken over the course of ten intensive observation periods (IOPs) during the month of July, 2003. Only data from IOPs 2 and 8 are used in this study. IOP 2 took place during the day and IOP 8 took place during the night. A complete description of the JU2003 experiment and the data is given by Allwine et al. [2004] and Clawson et al. [2005].

2. MODELS

The three models used in this study are the.Los Alamos National Laboratory's (LANL) QUIC model suite [Bagal et al., 2003], the Science Applications International Corporation (SAIC)–ARIA MicroSwift/Spray (MSS) model [Moussafir et al., 2004]; and the US Army Research Laboratory's (ARL) 3-Dimensional Wind Field (3DWF) model [Wang et al., 2005]. All models implement Röckle's original 1990 methodology but have been modified based on observations from a number of recent urban tracer studies and wind/water tunnel experiments. For example, QUIC has been updated to include new treatments for street canyon vortices, upwind rotor and displacement zones, and rooftop recirculation. Similarly, MSS now includes algorithms to merge cavity, wake, and upwind displacement zones. QUIC, MSS, and 3DWF all apply a variational mass conservation adjustment to the modified wind fields which assures near zero divergence in the 3-D solution.

Each of the modeling systems contains a Lagrangian particle dispersion model (LPDM) which uses the urban adjusted wind fields for transport and dispersion calculations. Because the Rockle models produce only simulations of the wind field and not the turbulence, it is necessary for the T&D models to parameterize the turbulent speeds and Lagrangian time scales for use in the LPDM. A thorough description of each modeling system can be found in the aforementioned references.

3. METEOROLOGICAL INPUTS

An abundance of meteorological data was collected and archived during JU2003. The wind data were collected using surface and rooftop sonic anemometers, radiosondes, and remote sounders such as RADARs and SODARs. The wind data used for model inputs in this study were 15-minute average vertical wind profiles collected with the Pacific Northwest National Laboratory (PNNL) SODAR, which was located in a suburban area approximately 3 km S/SW of downtown Oklahoma City. Wind directions were generally southerly and ranged from ~210 degrees during IOP 02 to ~157 degrees during IOP 08. The vertical resolution of the SODAR data was 10 m from 30 m to 500 m above ground level (AGL). Due to problems with the lower level data, only the SODAR observations at and above 100 m were used. Below 100 m, a neutral logarithmic profile was assumed using the relationship:

$$u_z = u_{100m} \times \left[\ln\left(\frac{z}{z_0}\right) \right] / \left[\ln\left(\frac{100}{z_0}\right) \right]$$

where z_o is the roughness length (assumed to be 0.5 m), z is the height, and u_{100m} is the SODAR wind velocity at z = 100 m. Zero displacement length is assumed and wind directions are set equal to the wind direction at 100 m. For each IOP, five 15-minute average profiles were constructed beginning 15 minutes prior to the tracer release to 1 hour after the beginning of the tracer release (e.g., 1545-1700 UTC for IOP 02.)

4. QUALITATIVE COMPARISON OF MODEL RESULTS AND FUTURE PLANS

An example of the near-surface wind outputs for IOP 2 is shown in Figure 2. In general, good first order qualitative agreement is found between the models. MSS and QUIC exhibit particularly good agreement with each other. Compared to MSS and QUIC, 3DWF seemed to create shorter wakes and showed an absence of skimming above similarly-spaced buildings. As a direct result, more trapping of release materials and

formation of concentration hotspots in building recirculation zones appears in MSS and QUIC results. Additionally, 3DWF appears to have greater advection, evidenced by generally lower concentrations and more rapid attainment of steady state, than do MSS and QUIC. This includes stronger channeling by 3DWF for IOP8, where free stream winds are more closely aligned with N/S streets.

Some issues such as upwind transport and dispersion by 3DWF, and some inconsistencies with concentration data, are still being investigated. Little upwind transport and dispersion is shown by QUIC and MSS.

While the simulation results varied somewhat between models, the results are similar and provide insight into the individual Röckle methodology implementations. Of course, no comparisons with observations have yet been made, so it is possible that all models have mean biases or that the one model that is an "outlier" actually agrees better with the data.

Future work will include continued model inter-comparisons for IOPs 02 and 08 including a more thorough quantitative comparison of model predictions to observations. There are observations from about 30 or 40 sonic anemometers in the model domain and we will compare the simulations and observations at those specific locations. The same type of quantitative comparison will be made using the 50 or 60 tracer samplers in the domain.

5. REFERENCES

Allwine, K. J., M. Leach, L. Stockham, J. Shinn, R. Hosker, J. Bowers, and J. Pace, 2004, Overview of Joint Urban 2003 – An atmospheric dispersion study in Oklahoma City, Preprints, Symposium on Planning, Nowcasting and Forecasting in the Urban Zone, American Meteorological Society, January 11-15, 2004, Seattle, Washington.

Bagal, N., E. Pardyjak, and M. Brown, 2003, Improved upwind cavity parameterization for a fast response urban wind model, AMS Conf. on Urban Zone, Seattle, WA, 3 pp.

Clawson, K. L., R. G. Carter, D. J. Lacroix, C. A. Biltoft, N. F. Hukari, R. C. Johnson, J. D. Rich, S. A. Beard, and T. Strong, 2005, Joint Urban 2003 (JU03) SF6 Atmospheric Tracer Field Tests, NOAA Tech Memo OAR ARL-254, Air Resources Lab., Silver Spring, MD.

Kaplan, H. and N. Dinar, 1996, A Lagrangian dispersion model for calculating concentration distribution within a built-up domain., Atmos. Environ., 30, 4197-4207.

Moussafir, J., O. Oldrini, G. Tinarelli, J. Sontowski, C. M. Dougherty, 2004, A new operational approach to deal with dispersion around obstacles: the MSS (Micro SWIFT SPRAY) software suite, 9th International Conference on Harmonization within Atmospheric Dispersion for Regulatory Purposes, June 1-4, 2004, Garmisch, Germany.

Röckle, R., 1990, Bestimmung der stomungsverhaltnisse im Bereich Komplexer Bebauugsstruckturen, Ph.D. thesis, Vom Fachbereich Mechanik, der Technischen Hochschule Darmstadt, Germany.

Rockle, R., 1994, Wind field and dispersion modeling in built-up areas, Proc of Lecture Series at ICTP, Trieste, Italy.

Wang, Y., C. Williamson, D. Garvey, S. Chang, and J. Cogan, 2005, Application of a multigrid method to a mass-consistent diagnostic wind model, J. Appl. Meteorol., 44, 1078-1089.

Williams, M., M. Brown, B. Singh, and D. Boswell, 2004 QUIC-PLUME Theory Guide, LA-UR-04-0561, 22 pp.

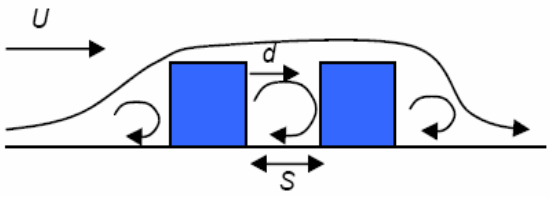

Figure 1. 2D street canyon schematic showing basic flow features (From Gowardhan and Pardyjak, 2005.)

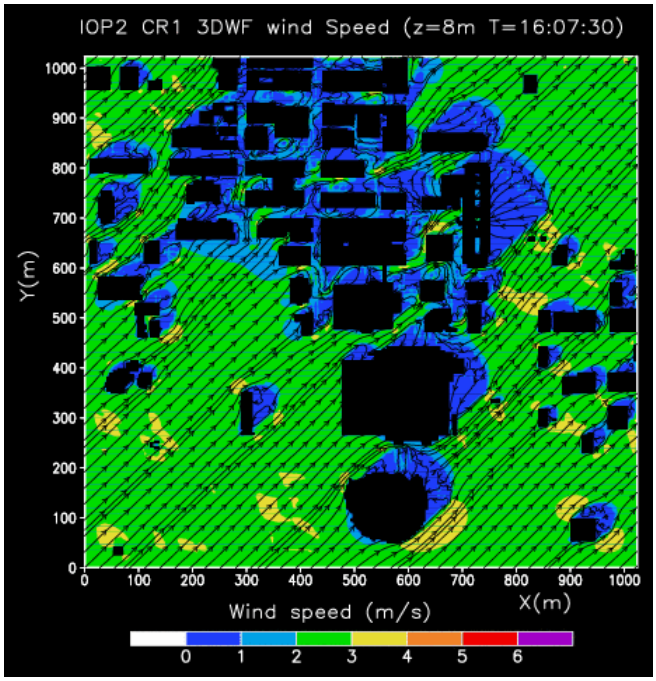

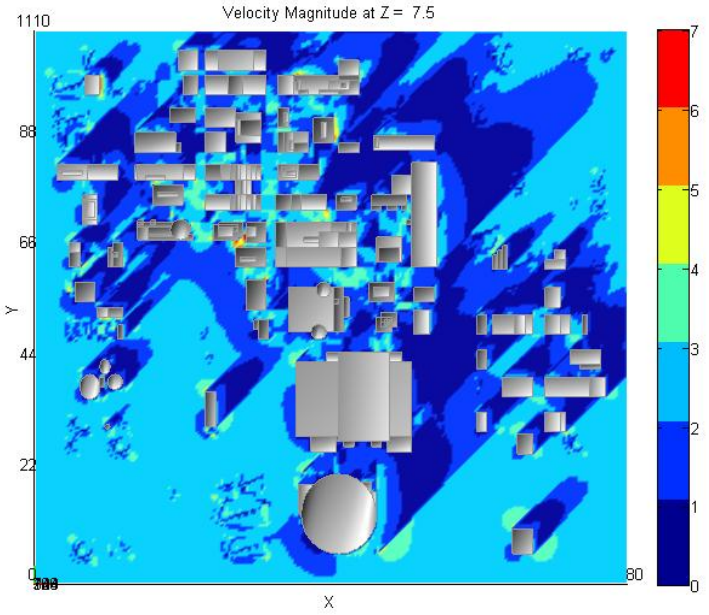

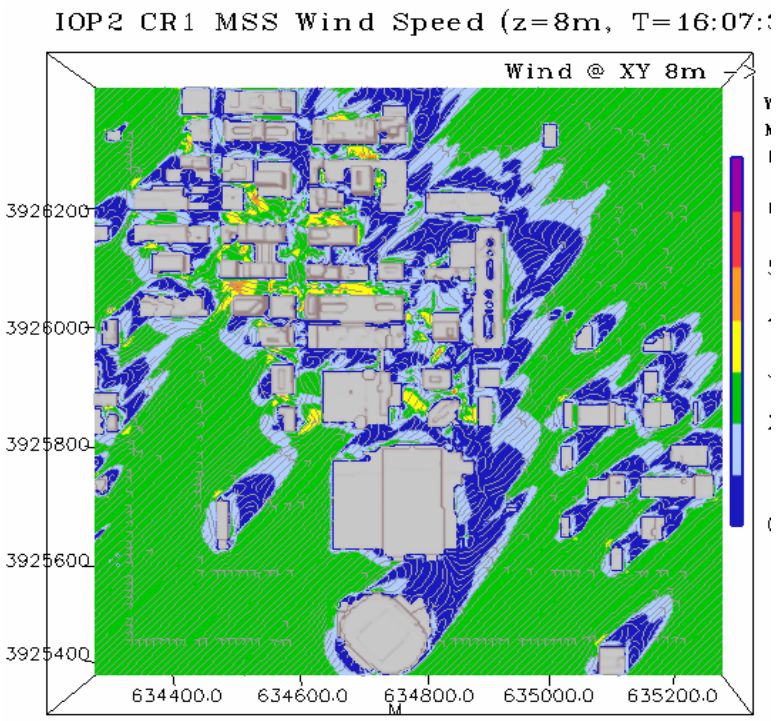

Figure 2. Example of 8m wind speed (m/s) plots for IOP02 for 3DWF, QUIC, and MSS, respectively.

Proceedings of the 6th International Conference on Urban Air Quality
Limassol, Cyprus, 27-29 March 2007

Impact of urbanisation on the some atmospheric variables in Akure, Ondo State, Nigeria

O. M Akinbode[1], A.O. Eludoyin[*2] and O. A. Ediang[3]

ABSTRACT

This study was carried out in one of the Administrative State Capitals in the southwestern part of Nigeria to highlight some effects of ubanisation on some climatic variables. Temperature and relative humidity data from 1992 to 2001 were obtained from the three meteorological stations, and the daily measurements taken along primary roads for 2 weeks. The results showed that the city is characterized annual mean temperatures, which ranged between 26.2^0C and 30.4^0C, and minimum and maximum temperatures that varied from 12.3^0C to 26^0C and 22.5^0C to 39.6^0C, respectively. The relative humidity ranged between 27.5% and 98.2%. Urban 'heat island' intensity was exhibited around central business district.

Keywords: *Temperature, Relative Humidity, Spatial and Temporal Variation, Spatial Distribution and Urban 'Heat Island'*

Introduction

Urbanization is not a recent phenomenon in Nigeria. What is peculiar however is the incidence of regional fragmentation in the urban areas. The central region often acquires the lion's share of the community's resource while the periphery suffers from inadequate resource allocation, relative underdevelopment and under-population (Onokerhoraye and Omuta, 1994). The city core, as a result of population concentration, intense transportation activity and surface concretization within it could therefore exhibit a microclimate different from other part of the same town, and giving rise to a condition of greater core temperature difference termed the urban 'heat island' intensity (UHI). The UHI is the characteristic warmth of urban areas compared to their (rural) surroundings. It is also often referred to as the increase of air temperature in the near - surface layer of the atmosphere within cities relative to their surrounding countryside (Voogt, 2002). It is so named because the isotherms forms an island shaped pattern. The built - up environment has been found to exacerbate heat stress, particularly at night, during heat waves and provides a preferential site for spread of vector borne diseases (Samuels, 2004).

This paper thus presents a preliminary assessment of the variations in the temperature and relative humidity in a Capital city in southwest Nigeria. The area has been selected because of its rapid urbanization from 1976 until present. The results presented are 10 years (1992 - 2002) of air temperature and relative humidity data from three established meteorological stations, and daytime, periodic, observations taken from 18 stations in the city in December 2002. The study is important because the microclimate of Nigerian cities has not been well documented, and little is known about their effects, especially in the growing state capitals, which form the present focus of socio-economic growth in the country.

[1] Department of Geography and Planning Sciences, Adekunle Ajasin University, Akungba Akoko, Ondo State, Nigeria
baynick2003@yahoo.com
[*] Corresponding author
[2] Department of Geography, Obafemi Awolowo University, Ile - Ife, Nigeria, **oaeludoyin@oauife.edu.ng**
[3]

Materials and Methods

Sample design, collection, and field observations

Field data were collected in December 2002. 27 sampling stations were established based on the land use map of Akure: three from each of Oke - Aro, and Araromi districts (residential), Oba, Isikan and NEPA markets (commercial), COOP (industrial), Oba Ile and Owo roads (vegetated and relatively undisturbed sites), and Ondo – Ore Motor Park. Temperature and relative humidity readings were also obtained at road junctions, under overhead bridges and open spaces to reflect the various characteristics of the roads in 9 stations, along the 2 primary (Ilesa to Oba – Ile and Ondo to Igbatoro) roads that traverse the city. The instrument used for the daytime temperature and relative humidity was the sling psychrometer, consisting of both a dry and wet bulb thermometer.

Results and Discussion

This investigation aimed at assessing the impact of urbanisation on the relative humidity and temperature in Akure, Nigeria. The higher temperature and lower relative humidity observed in the commercial area compared to that obtained at the countryside, as seen in this study is similar to the pattern obtained in cities in other countries such as Dhaka, Bangladesh (Hossain and Noorudin, 1994), Brazil (Maitelli *et al*, 2003) and Beijing, China (Svensson and Tarvainen, 2004). From this study, urbanisation played a significant role in the distribution of temperature and relative humidity. The Motor Park and commercial areas have higher mean average temperature than the outskirts. These two areas also exhibited lower relative humidity. Similar patterns of temperature and relative humidity were demonstrated in the temperature changes along the two major roads, which traversed the city. The areas at the interior of the city were generally warmer than the exterior. Oke (1987) suggested that the structure and composition of the urban canopy and the thermal properties of urban construction materials are the main factors that determine the urban - rural thermal contrasts. The fact that urban areas tend to be warmer has been well studied and documented (e.g. Oke, 1982; Arnfield, 2003; Samuels, 2004; Svensson and Tarvainen, 2004).

It is also known that the higher temperatures are often associated with higher density urban dwellings, where it forms an urban heat island. The daytime 'heat island' intensity at the time of this study was however less than those of Dhaka, Bangladesh (5^oC - 6^oC) (Ayesha, 1995), Ibadan, Nigeria (4^oC - 8^oC) (Oguntoyinbo, 1982), Benin City (4^oC), Nigeria (Omogbai, 1985) The relatively small amount of the daytime heat island in this study falls within the range observed in Ibadan in December (Oguntoyinbo, 1986). The difference in the urban heat intensity in this study from other areas may be explained by the phenomenon at the daytime hours in which this study was conducted (Runnalls and Oke, 2000). The main 'heat island' characteristics described in some studies (Voogt, 2002) were also observed in Akure at the time of this study. The CBD contains closely spaced buildings and most of the buildings ranged from 2 to 4 storey buildings, open market spaces where over 10, 000 people trade daily. These form the thermal sinks and urban hot spots (Bornstein and Lin, 1999), which could absorb and emit heat – the active ingredient in generating the urban heat island phenomenon (Samuels, 2002).

The results of the One - way Analysis of Variance performed separately on each land use type suggested that the mean temperature did not vary significantly at different locations within the city. The relative humidity did show significant variation. Generally, there was relative uniformity in the mean temperature in Akure while the distribution of the relative humidity suggested local influence. For example, less humid surfaces were obtained in the commercial areas and Motor Park. This result is similar to that obtained in the two cities of Cuiaba and Verzea Grande in Brazil (Maitelli, *et al*,

2003) in which the temperature trend was found to be inversely proportional to the relative air humidity. The outskirt of Akure is semi - urban settlement with high indexes of vegetation cover. The relative humidity in this environment has largely been accounted for by the higher rate moisture release from transpiring vegetation. In addition, diurnal variation existed in both the temperature and relative humidity fields within the city. The trend is similar to those obtained in Dhaka, Bangladesh (Ayesha, 1995) where 1500 hour was the warmest. While temperatures in the city generally increased from 0900 to 1500 before they declined towards the 1800 LST, its relative humidity has decreased.

The findings revealed the need for more archival data on temperature before adequate monitoring could be made for any meaningful remedial intervention. The need for a good network of well-equipped meteorological stations to improve the climate study in this city cannot be over-emphasized. At present, the quality of the city atmosphere requires that urban growth should be monitored.

REFERENCES

Adebayo, Y.R. (1985) The Microclimatic Characteristics within the Urban Canopy of Ibadan, Unpublished PhD Thesis, Department of Geography, University of Ibadan, Nigeria.

Arnfield, A. J. (2003) Two Decades of Urban Climate Research: A Review of Turbulence, Exchanges of Energy and Water, and the Urban Heat Island, *International Journal of Climatology,* 23: 1 – 26.

Bornstein, R. and Lin, Q. (1999) *Urban Convergence Zone Influences on Convective Storms and Air Quality*, Congress of Biometeorology and International Conference on Urban Climate, WMO, Sydney, Nov.

Hossain, M.E. and Nooruddin, M. (1994) *Some Aspects of Urban Climates of Dhaka City* In: Reports of the Technical Conference on Tropical Urban Climates, March 28 – April 2, 1993, Dhaka, Bangladesh.

Maitelli, G. T., Souza, S. C. and de Pinho, J. G. (2002) *The Magnitude of Urban Heat Island in the Tropical Continental Areas in Brazil*, Department of Geography, University of Mato Grosso, Brazil 1 - 4.

Oguntoyinbo, J.S. (1982) *Climate Characteristics* In: Filani, M.O. (ed.) Ibadan Regions. Department of Geography, University of Ibadan, Nigeria

Oke, T.R. (1982) The Energetic Basis of the Urban Heat Island, *Quarterly Journal of the Royal Meteorological Society* 108: 1 - 24

Oke, T.R. (1987) Boundary Layer Climates, Methuen, London

Omogbai, B.E. (1985) Some Aspects of Urban Climates of Benin City, Nigeria, Unpublished M.Sc. Thesis, University of Ibadan, Nigeria.

Onakerhoraye, A. G. and Omuta, G. E. (1994) Urban Planning Systems and Planning for Africa, Benin Social Science Series for Africa, University of Benin, Nigeria.

Runnalls, K. E. and Oke, T. R. (2000) Dynamics and Control of the Near – Surface Heat Island of Vancouver, British Columbia, *Physical Geography*21 (4): 283 – 304

Samendra, K. and Ayesha, K. (1994) *The Variability and Probability Extremes of Some Climatic Elements Over Dhaka*, Reports of the Technical Conference on Tropical Urban Climate, March 28 – April 2, 1993, Dhaka, Bangladesh.

Samuels, R. (2004) *Urban Heat Islands*, Australian House of Representative Standing Committee on Environment and Heritage Sustainable Cities 2025 Enquiry.

Santamouris, M. (2001) *The Canyon Effect*, In: Santamouris, M. (ed.) Energy and Climate in the Urban Built Environment, James and James, London.

Svensson, D and Tarvainen, L. (2004) The Past and Present Urban Heat Island of Beijing, B416 Projektarbete Goteborg, Earth Sciences, Goteborg University, Sweden.

Voogt, J. A. (2002) Urban Heat Island In: Munn, T. (ed) Encyclopedia of Global Change, John Wiley and Sons, 660 - 666.

DEVELOPMENT OF GAMMA-MET ON SENSIBLE HEAT CALCULATION FOR URBAN CHARACTERISTIC: CASE STUDY BANGKOK, THAILAND

Surat Bualert

Faculty of Science, Chulalongkorn University, Bangkok 10330, Thailand

ABSTRACT

GAMMA-MET's performance could be enhanced by using onsite parameters for Bangkok to improve the model's boundary layer parameters. Ordinary meteorological pre-processors use Bowen ratio and its default value to calculate sensible heat flux, However, Thailand has a different climate from northern latitude countries where the Bowen ratio was first applied in dispersion model. Therefore, development of an appropriate sensible heat flux calculation was conducted in this research.

Thai meteorological stations were used to study the urban Bowen ratio The profile measurements were used to calculate sensible heat flux and compared to eddy covariance method. The Bowen ratios were 3.95 to 5.61. Sensible heat flux calculated by Bowen ratio gave 29 % lower than the eddy covariance method. Furthermore, the Bowen ratio was applied for sensible heat flux calculations within GAMMA-MET. The results showed a good agreement of these sensible heat flux calculations with eddy covariance results at Chalumprakia meteorological station.

KEYWORDS

Sensible heat flux, Latent heat flux, Meteorological preprocessor, Urban meteorology, Bowen ratio

1. INTRODUCTION

Dispersion models need meteorological parameters as input data to describe the dispersion conditions. The boundary layer parameters such as friction velocity, and heat flux should take into account the effects of physical and thermal properties. These parameters can be used to identify atmospheric stability as the Monin-Obukhov length, which is more efficient than traditional methods which described stability conditions by stability classes, e.g. Pasquill-Gifford stability classification. However, these parameters need more site specific information and are not routinely measured by normal surface synoptic meteorological stations. Sensible heat flux is the parameter that is affected by thermal property of land cover around the measured site. Latent heat flux is influenced by the extent of free surface water and vegetated areas within the city. There are two major methods used for sensible heat calculation, Bowen ratio and eddy covariance.

The sensible heat flux used for the Monin-Obukhov length was calculated via a Bowen ratio method which used the default values in the model. These default urban values were 1.0-4.0. However, when the model was applied to the different environment and location such as Bangkok, the default values may not be suitable. Therefore, development of the GAMMA-Met sensible heat calculation was conduced in Bangkok, Thailand.

2. METHODOLOGY

2.1 Meteorological measurements

Bang-Na and Chalumprakia meteorological stations in Bangkok were used as study areas. The measurements were conducted over three seasons, summer, winter and rainy season in 2005 (Table 1). Ambient air temperature, soil temperature, global solar radiation, atmospheric pressure, relative humidity and wind component were measured by using WMO standard equipments.

Table 1 measurement periods

Stations	Season		
	Rainy	Winter	Summer
Bang-Na station	May 2005	Jan 2005	April 2005
Chalumprakia station	May 2005	Dec 2004	April 2005

(1) Ambient air and Soil temperature were measured at different levels (1.2m 0.5m, 0m, -0.05m, -0.20m) and were recorded by using a micro-data logger.

(2) Wind component was measured by using 3D-Sonic anemometer.

(3) Collect global solar radiation, atmospheric pressure and relative humidity from routine meteorological data.

(4) Calculate Bowen ratio (Wiesner, 1970), latent heat of evaporation (Oke, 1978) and (Lockwood, 1974) and sensible heat (USEPA, 1999).

(5) Compare sensible heat flux from Bowen ratio with that measured by the eddy covariance method.

2.2 Study Area

1) Bang-Na meteorological station is operated by Royal Thai meteorological department located in Bangkok. Surrounding land covers of Bang-Na station are green area, constructed area, water surface, and roads: around 48.5, 44.50, 3.51 and 3.47 percent of the 1 km^2 near to the station, respectively.

2) Chalumprakia meteorological station operated by Royal Thai meteorological department located in Bangkok. Surrounding land covers of Bang-Na station are green area, constructed area, water surface, and road around 17.33, 68.15, 9.7 and 4.82 percent of the 1 km^2 near to the station, respectively.

3. RESULTS and DISCUSSION

3.1 Bang-Na meteorological station

3.1.1 Heat flux calculated by Bowen ratio

(1) Calculated Latent heat fluxes were 221.84, 171.79 and 243.56 watt per $meter^2$. in rainy winter and summer season respectively (Table 2).

(2) Surface heat fluxes were 8.25, 72.62 and 66.98 watt per $meter^2$ in rainy, winter and summer respectively (Table 2).

(3) Sensible heat fluxes were high in winter and summer, 96.72 and 243.56 watt per $meter^2$, respectively. In the rainy season, the sensible heat flux was 0.96 watt per $meter^2$, lower than in winter or summer (table 2)

3.1.2 Heat flux measured by eddy covariance method

(1) Measured latent heat flux was highest in rainy season, 140.7 watt per $meter^2$. During winter and summer, averaged latent heat flux was 56.86 and 59.71 watt per $meter^2$, respectively (Table 3).

(2) Surface heat flux was 7.47, 11.88 and 4.48 watt per $meter^2$ in rainy, winter and summer respectively (Table 3).

(3) Measured sensible heat flux was high in winter and summer, averaged 272.63 and 282.87 watt per $meter^2$, respectively. Rainy season, the sensible heat flux was 129.08 watt per $meter^2$, lower than winter and summer (Table 3).

Table 2 Averaged net solar radiation, sensible heat flux , latent heat flux and surface heat flux calculated by using Bowen ratio method at Bang-Na meteorological station during sampling period in year 2005.

Parameters	Rainy	Winter	Summer
R_n (W m^{-2})	219.37	380.78	415.12
H (W m^{-2})	0.96	135.26	104.57
LE (W m^{-2})	221.84	171.79	243.56
X (W m^{-2})	8.25	72.62	66.98
Bowen ratio	0.02	1.74	1.21

Table 3 Averaged net solar radiation, sensible heat flux, latent heat flux and surface heat flux calculated by using Eddy correlation at Bang-Na meteorological station during sampling period in year 2005.

Parameters	Rainy	Winter	Summer
R_n (W m^{-2})	277.25	340.45	347.07
H (W m^{-2})	129.08	272.63	282.87
LE (W m^{-2})	140.7	56.86	59.71
X (W m^{-2})	7.47	11.88	4.48
Bowen ratio	3.33	6.38	6.55

Comparison of latent heat flux between two methods show that Bowen ratio method tends to give under-prediction (around 29 %) compared to eddy's covariance method, but it shows a good relationship. The reason should be the atmospheric condition of the study area because the Bowen ratio method was suitable for neutral conditions and a natural environment. For the urban area, physical and man-made environments are dominant. Therefore, the latent heat was limited by amount of water in the air. In addition, 1.2m height of air temperature may not show a clearly difference to surface temperature.

3.2 Chalumprakia meteorological station

The Bowen ratio calculated by using measured meteorological data at Bang-Na station was used to calculate the sensible heat at Chalumprakia station. The sensible heats were lower than sensible heat measured by eddy covariance method. Therefore, sensible heat and latent heat calculated by eddy covariance method were used to calculate Bowen ratio.

(1) Latent heat of evaporation flux was highest in rainy season, 109.32 watt per $meter^2$. During winter and summer, averaged latent heat was 53.14 and 226.66 watt per $meter^2$, respectively (Table 4)

(2) Surface heat flux were 4.28, 7.82 and 7.5 watt per $meter^2$ in rainy, winter and summer respectively (Table 4).

(3) Sensible heat flux were 296.27, 231.68 and 251.14 watt per $meter^2$, in rainy , winter and summer season respectively (Table 4).

Table 4 Averaged net solar radiation, sensible heat, latent heat and surface heat calculated by using Eddy correlation at Chalumprakia meteorological station during sampling period in year 2005.

Parameters	Rainy	Winter	Summer
R_n (W m^{-2})	409.88	292.64	485.3
H (W m^{-2})	296.27	231.68	251.14
LE (W m^{-2})	109.32	53.14	226.66
X (W m^{-2})	4.28	7.82	7.5
Bowen ratio	4.15	6.71	2.55
Bowen ratio (Bang-Na station)	3.33	6.38	6.55

3. 3 Application of GAMMA-MET on Chalumprakia meteorological station

GAMMA-MET was used to calculate sensible heat flux during winter and summer season at Chalumprakia meteorological station by using Bang-Na's Bowen ratio (6.38 and 6.55 for winter and summer). The result was compared to eddy covariance method. The result showed that calculated sensible heat flux gave a good agreement to the eddy covariance method. It was 65.9% within factor of two and Bowen ratio gave over prediction (Figure 1).

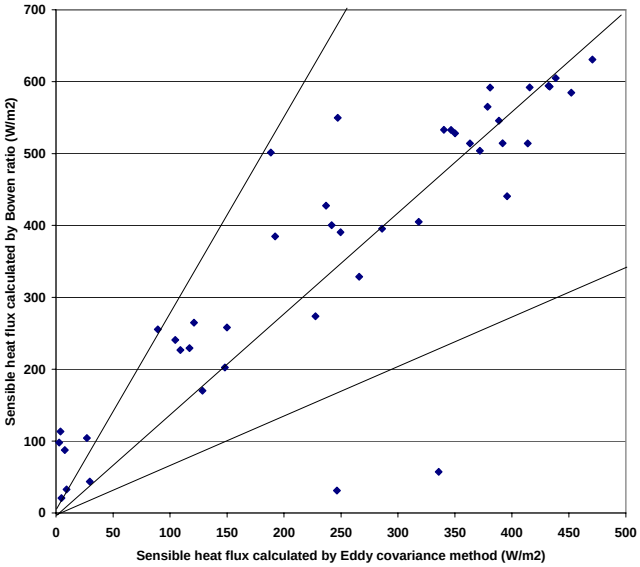

Figure 1 Comparison of sensible heat flux calculated by eddy covariance method and Bowen ratio at Chalumprakia meteorological station

Bowen ratio method and eddy covariance method can be used to calculated sensible heat flux and latent heat flux. The first parameter, Bowen ratio, can be used as a constant when meteorological instruments were not available. The constant or Bowen ratio has been used in referenced meteorological preprocessor, AERMET, PCRAMMET. Therefore, in case of Bangkok, Thailand, Bowen ratio was different from default value in the models. In addition, there were some errors of the calculation when calculated by Bowen ratio method, especially in very unstable condition. The calculation gave a negative latent heat and sensible heat flux. That caused by the Bowen ratio was suitable in neutral condition.

4. CONCLUSION

1) Eddy covariance method is a suitable method for calculating sensible heat flux and latent heat flux in urban environment.
2) Meteorological pre-processor can use Bowen ratio to calculate sensible heat flux but it need to consider location and climate of application site.
3) GAMMA-MET, meteorological pre-processor model has been applied to Bangkok using a locally derived Bowen ratio to calculate the sensible heat flux.

5. ACKNOWLEDGEMENT

The meteorological data was received from Meteorological Department of Thailand. Their assistance is gratefully acknowledged.

6. REFERENCES

Lockwood, J. G. 1974. World climatology: An environmental approach. London: Edward Arnold.

Oke, T. R. 1978. Boundary layer climates. New York: John Wiley & Sons.

USEPA.: 1999. User's guide for the AERMOD Meteorological Preprocessor (AERMET). Office of Air Quality Planning and Standards Emissions, Monitoring, and Analysis Division Research, Triangle Park.

Wiesner, C. J. 1970. Hydrometeorology. 1st ed. London: Chapman and Hall.

THE MIXING HEIGHT DETERMINATION IN TESTBED CAMPAIGN IN HELSINKI, FINLAND

N. Eresmaa[(1)], A. Karppinen[(1)], K. Bozier[(2)], M. Rantamäki[(1)]

(1) Finnish Meteorological Institute
(2) University of Salford, Great Britain

ABSTRACT
The data utilized in this study has been collected during Helsinki Testbed research project in Helsinki metropolitan area. We have tested different techniques on mixing height (MH) estimation based on the data obtained from 5 ceilometers, a Doppler lidar, a radio acoustic sounding system (RASS) and radiosoundings. The radisoundings have been considered as the reference method on mixing height determination. On the ceilometer and Doppler lidar data we have tested a new 3-step method, which seems to be quite promising with the ceilometer. With the Doppler lidar data a fixed threshold method worked better. In this research the RASS was the weakest instrument on the MH estimation as it reported values only between 140 and 700 meters.

1. INTRODUCTION

Helsinki Testbed is a research project of mesoscale meteorology running for two years and a half, from January 2005 until September 2007 in Helsinki metropolitan area (http://testbed.fmi.fi/). Among all the measurement systems the campaign is equipped with 7 ceilometers, a Doppler lidar (Bozier et al., 2007) and a radio acoustic sounding system (RASS). In addition to these measurements also radiosoundings are performed occasionally. The ceilometers (operating at the wavelength of 910 nm) and the Doppler lidar (wavelength 1.55 μm) observe the aerosol backscattering profile; the lidar also provides us the radial wind velocity data. The RASS and radiosoundings measure the temperature profiles.; radiosoundings provide also the wind and humidity profiles.

We have utilized data from 5 different measurement spots: 2 urban, 1 suburban and 2 rural sites. The map of measurement sites is shown in figure 1. The simultaneous measurements provide us a good opportunity to compare different methods and measurements with each other. Also, because of several measurement sites, it is possible to examine the spatial variation of mixing layer in different surroundings.

Figure 1. *The map of Testbed measurements. All the measurement sites have a ceilometer; the RASS is situated in Malmi and the radiosoundings are performed in Vantaanlaakso.*

One big problem in comparing the different methods was the scarcity of simultaneous measurements. All of the investigated data had large gaps which complicated this task. In this research we have used 2 periods of observations. The first study period (one day) was at 22nd of November 2005; the second period was from 9th August to 28th August 2006. During both of the periods the air quality in Helsinki metropolitan area was poor: during the first period due to a surface inversion and during the second period due to regional range transport originating from wild land fires in Russia.

2. METHODOLOGY

For obtaining the reference mixing height we have treated the radiosounding profiles in two ways: In all cases the mixing height is determined using the Richardson method (Joffre et al., 2001) with the critical number of one. The daytime soundings have also been scrutinized with the Holzworth method (Holzworth 1964, 1967) where the principle is to follow the dry adiabate starting at the surface up to its intersection with the actual temperature profile.

Since in general aerosol concentrations are lower in the free atmosphere than in the mixing layer, the MH can be associated with a strong gradient in the vertical backscatter profile. Earlier Steyn et al. (1999) and Eresmaa et al. (2006) have used an idealized backscatter profile method to determine the mixing height based on the ceilometer data. This method, however, had to be revised because of the differences between used in this and the previous study. The revised method is an extension of the original idealized backscatter method with 3 steps: A profile *B(z)* is fitted to the measured profile by the formula

$$B(z) = \underbrace{\frac{B_1 - B_{ML}}{2} - \frac{B_1 - B_{ML}}{2} erf\left(\frac{z - MH_1}{\Delta h_1}\right)}_{STEP1} + \underbrace{\frac{B_{ML} - B_2}{2} - \frac{B_{ML} - B_2}{2} erf\left(\frac{z - MH_{ML}}{\Delta h_{ML}}\right)}_{STEP2} + \underbrace{\frac{B_2 + B_U}{2} - \frac{B_2 - B_U}{2} erf\left(\frac{z - MH_2}{\Delta h_2}\right)}_{STEP3}$$

where B_1 corresponds to the backscattering at the surface, B_{ML} is the mean mixing layer backscatter, B_2 corresponds to backscattering above the mixing layer and B_U is the mean backscatter of the free atmosphere. MH_i corresponds to the height of the step i, and Δh_i is related to the thickness of the gradient zone. An example of the fitting is illustrated in figure 2.

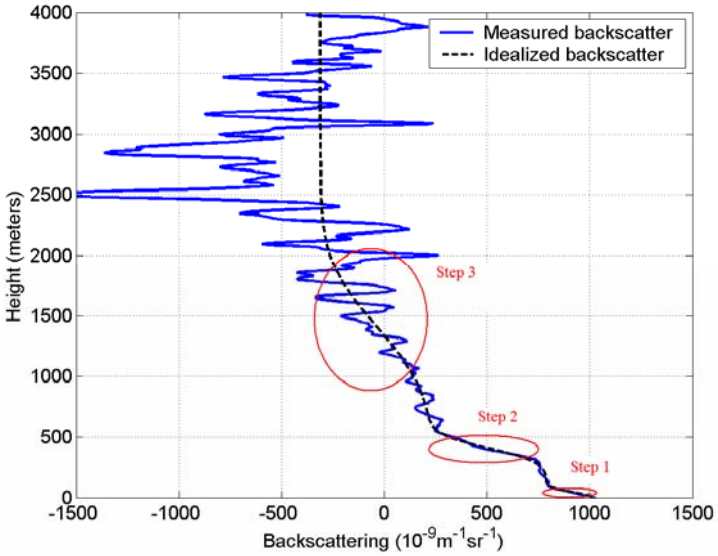

Figure 2. *An illustration of the idealized backscattering profile (Vallila, 21 August 2006 at 11UTC).*

The same idealized backscatter method is applied to the lidar data. We have also experimented with other methods to determine the mixing height, i.e. method based on the observed height of the backscatter maximum and method based on the height where the backscatter falls below a fixed threshold value. The comparison was made against mixing heights determined by ceilometer. An example of the Doppler lidar backscatter profile is illustrated in figure 3.

The first measurement gate of RASS is the height of ca. 150 meters, thus operational MH determination based solely on RASS is practically impossible. The only situations where RASS profiles were found to be useful were the surface inversions – and even in these cases it must be kept in mind that the height of inversion is not necessarily directly related to the mixing height.

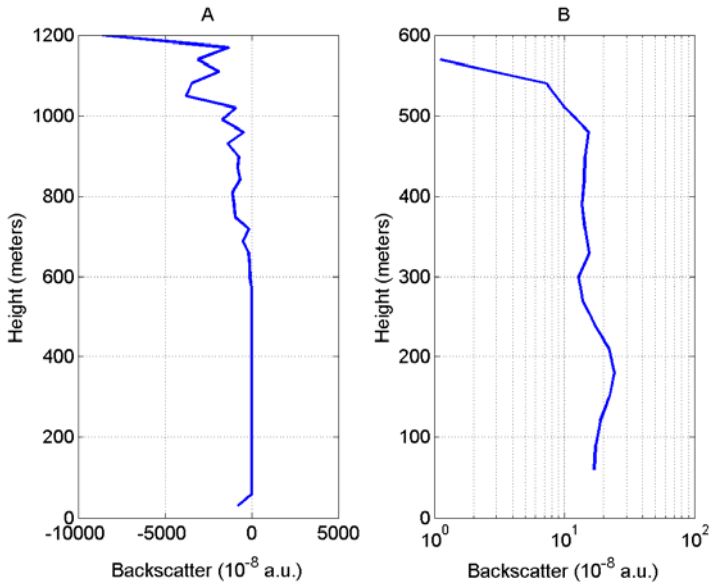

Figure 3. *An example of the lidar backscatter profile. In figure A the whole measurement range is shown; figure B illustrates the backscatter in the lowest 600 meters.*

3. RESULTS AND DISCUSSION

The comparison between measurement sites showed no significant differences between urban and rural areas.

The number of observations in the comparison of ceilometer and radiosoundings is small; only 12 clear sky cases were analyzed. This is mainly due to difficult weather conditions: low clouds dominated the second observation period while during the first observation period the radiosounding profiles were not yet available.

The correlation between MHs determined by the reference method (radiosoundings) and ceilometer is 0.62 (t=2.50; p > 97.5 %); corresponding regression line (with 95 % confidence limits) is

$$h_{ceilometer} = (0.66 \pm 0.60) h_{sounding} + (230 \pm 260)$$

An example of a full 24-h period of ceilometer observations is presented in figure 4. It can be seen clearly how turbulence grows stronger and the MH grows as the sun rises. On the other hand, the loss of echo intensity after the smog situation (echo is missing appr. from 14 UTC until 17 UTC) provides a good illustration of a potential problem using this method operationally. In this case the algorithm provided us some realistic values, but in some other similar cases the algorithm does not work at all. Fig. 4 also shows examples of rain events (appr. 6:30 UTC and 19:30 UTC) when the MH determination based on ceilometers is not possible.

The comparison between the MHs estimated by ceilometer and Doppler lidar shows that the most promising way to estimate MH from the Doppler lidar data among the investigated method is the fixed threshold value method (see Table 1). The utilization of the idealized 3-step method is difficult because of the fractional changes of the backscatter intensity in the boundary layer.

Table 1. *The comparison between MHs determined by ceilometer and three investigated Doppler lidar methods*.

	Correlation coefficient	Regression line
Fixed threshold value (10^{-7})	0.71	$MH_{lidar} = (0.90 \pm 0.37) MH_{ceilometer} - (18 \pm 170)$
Idealized 3-step method	-0.06	$MH_{lidar} = (0.30 \pm 0.14) MH_{ceilometer} + (560 \pm 65)$
Height of the backscatter maximum	0.35	$MH_{lidar} = (0.20 \pm 0.44) MH_{ceilometer} + (660 \pm 68)$

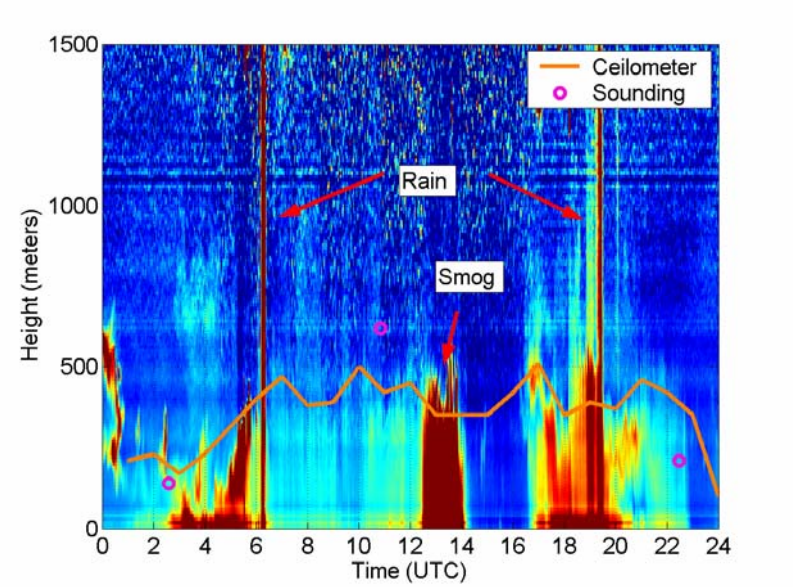

Figure 4. *A 24-h period of ceilometer echo intensity observations at Vallila, Helsinki, 21 August 2006. The height of the MHs determined by the ceilometer and Richardson number method are superimposed on the ceilometer raw echo data.*

Surface inversions occurred only during the first case. RASS based MH estimates compared very well the reference method (radiosoundings), however, more data is needed to make statistically reliable conclusions.

4. CONCLUSIONS

We have examined methods to determine the mixing height utilizing three different measurement systems, i.e. ceilometer, Doppler lidar and RASS. Radiosoundings have been used as the bases for the reference method. The results show that none of the measurement systems alone is good enough for operational mixing height determination.

The most promising methods for mixing height determination are the ceilometer and the Doppler lidar. Both systems still face some problems. The biggest problem for ceilometer are the cloudy and rainy conditions, whereas the biggest problem for the lidar is the limited height of the data – the data above 600 meters was in the studied cases dominated by noise.

5. REFERENCES

Bozier, K., Pearson, G. N. and Collier, C. G., 2007: Evaluation of a new autonomous Doppler lidar system during the Helsinki Testbed field campaign. American Meteorological Conference, Third Symposium on Lidar Atmospheric Applications, San Antonio, Texas, USA, 15-18 January 2007.

Eresmaa, N., Karppinen, A., Joffre, S. M., Räsänen, J. and Talvitie, H., 2006: Mixing height determination by ceilometer. *Atmospheric Chemistry and Physics*, **6**, 1485-1493

Holzworth, C. G., 1964: Estimates of mean maximum mixing depths in the contiguous United States. *Monthly Weather Review*, **92**, 235-242

Holzworth, C. G., 1967: Mixing depths, wind speeds and air pollution potential for selected locations in the United States. *Journal of Applied Meteorology*, **6**, 1039-1044

Joffre, S. M., Kangas, M., Heikinheimo, M. and Kitaigorodskii, S. A., 2001: Variability of the stable and unstable atmospheric boundary-layer height and its scales over a boreal forest. *Boundary-Layer Meteorology*, **99**, 429-450

Steyn, D. G., Baldi, M. and Hoff, R. M., 1999: The detection of mixed layer depth and entrainment zone thickness from lidar backscatter profiles. *Journal of Atmospheric and Oceanic Technology*, **16**, 953-959

Proceedings of the 6th International Conference on Urban Air Quality
Limassol, Cyprus, 27-29 March 2007

AIR POLLUTION METEOROLOGY – A CASE STUDY OF SWANSEA, UK

T. Habeebullah[1], S. Dorling[1] and P.Govier[2]

[1] School of Environmental Sciences, University of East Anglia, UK
[2] City and County of Swansea, Environment Department, Swansea, UK

ABSTRACT

Urban areas can have significant influence on local microclimate. Further complications may occur if urban areas are located in complex topography. Swansea, on the South Wales coast, is surrounded to the north by higher ground. There are therefore many things to consider when diagnosing or forecasting localised weather conditions in the city and therefore the dispersion and removal of air pollutants. Unusually, meteorological measurements are made at multiple city locations. Furthermore, a 30m mast and sodar instrument are being installed to better understand the vertical wind profile. A local air quality NO_2 and PM_{10} management area has been declared in one part of the city.

We present an analysis of inter-annual variability of the local climate of Swansea, plus an inter-comparison between urban, sub-urban and surrounding rural weather measurements. We also evaluate the accuracy of mesoscale model weather forecasts as part of an integrated urban air quality forecasting system.

INTRODUCTION

It is rare to have access to long time-series of meteorological measurements at multiple locations across a city. In fact, urban air pollution modellers are often faced with utilising meteorological measurements from a nearest station some kilometres outside the city, for example at an airport well away from the urban centre. It is usually only during short intensive research campaigns that the meteorological heterogeneity within an urban area begins to be revealed.

Swansea, on the South Wales coast (Figure 1), is therefore rather unusual. In addition to a nearby rural synoptic weather station, located at the very exposed headland known as Mumbles Head, meteorological measurements are also made at three air quality monitoring stations in the city, at the Guild Hall, at Morfa and at Morriston. As a way of highlighting the impact that choice of weather station can have on air pollution dispersion in an urban environment, this paper compares and contrasts the meteorological measurements made at the aforementioned stations, focusing in particular on air temperature, wind speed and direction. A 30m mast and sodar instrument, presently being installed and deployed, will add further to our knowledge of how the microclimate varies both horizontally and vertically.

An air quality management area (AQMA), in the Hafod area of the city, has been established in order to address air quality problems relating to NO_2 and PM_{10}; traffic is a major contributor to the poor air quality, despite local attempts to alleviate the problem through, for example, Park and Ride schemes. An integrated air quality modelling and management system is being developed, incorporating a weather forecast, to ultimately provide the ability to manage air quality on a realtime basis. Weather forecasts are provided from the mesoscale model of the Danish Meteorological Institute (DMI) and we assess here how closely such a model can simulate the complex conditions experienced across an urban area. The challenge is made all the greater by the topographic complexity of the local environment, with both local coastal and terrain effects.

METHODOLOGY

Our approach here is a simple one, just to compare the meteorological data for the year 2005 between stations, in the form of seasonal cycles of temperature and of wind roses. We also present statistics quantifying the degree of accuracy of the mesoscale model forecasts for the same year, including forecasts of different time horizon from T+6 hours to T+72.

Figure 1: Location of meteorological and air quality monitoring stations in and around the city of Swansea.

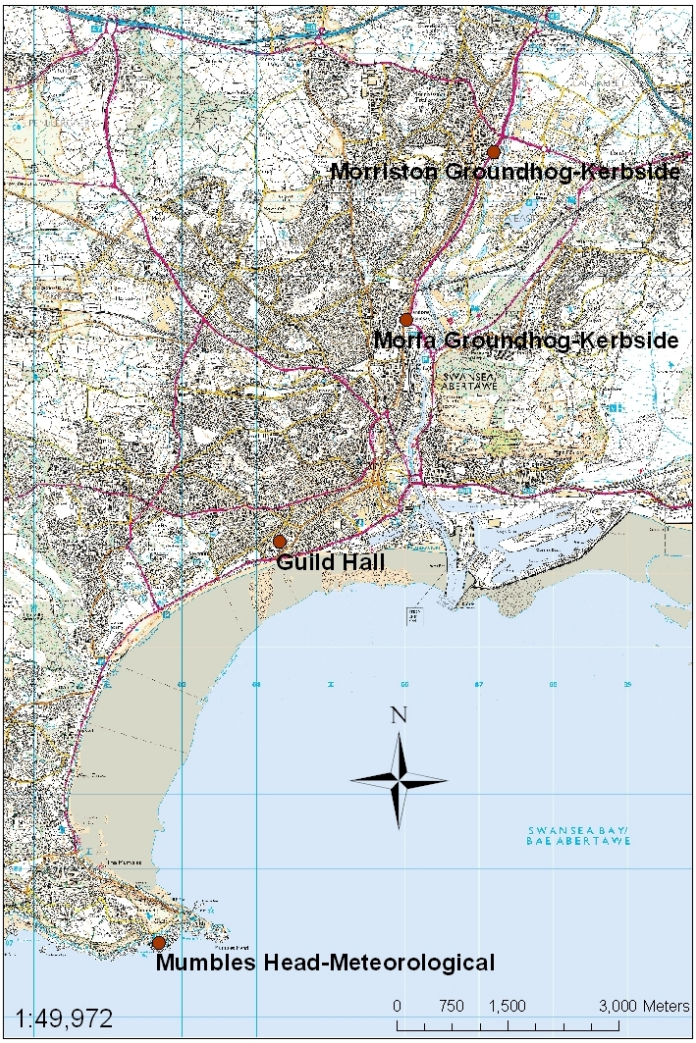

RESULTS AND DISCUSSION

Figure 2 shows the seasonal cycle of air temperature, during 2005, at the four meteorological monitoring stations. The outstanding feature is the urban heat island displayed at the Guild Hall station. Interestingly, in the autumn and early winter, it is clear that the relative warmth of the sea, at that time of year, reduces the temperature difference between the Guild Hall and the exposed Mumbles Head. Also notable is that Morfa is the coldest of the stations, least influenced by urban temperature increments and coastal effects.

Table 1 breaks the data down further, showing how air temperature varies between stations at both midday and midnight during 2005. These results emphasize the larger urban effect at night, with the air temperature averaging as much as 4.3C higher at the Guild Hall than at Morfa.

Table 1: Comparison of the 12z and 00z air temperature (^{o}C) between Morriston, Morfa and the Guild Hall during 2005

Statistics	Morriston - Morfa	Morriston – Guild Hall	Morfa – Guild Hall
Bias (12z)	1.9	-1.1	-3.0
Bias (00z)	2.4	-1.9	-4.3

Figure 2: Comparison of the seasonal cycle of monthly average air temperature between monitoring stations during 2005.

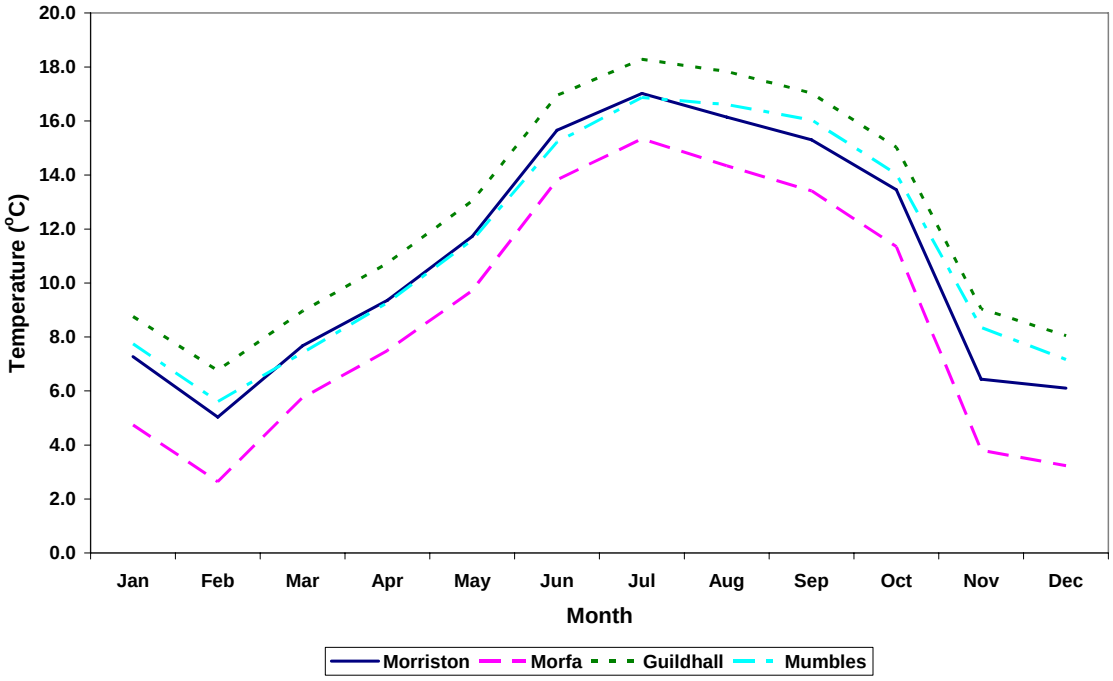

Figure 3 presents the wind roses for the same set of four stations. It should first be noted that wind measurements are made at a height of 6m at Morfa and Morriston and at 10m at the Guild Hall and at Mumbles Head. Substantial differences can be noted between stations, both in terms of wind speed and direction. The more exposed Mumbles Head exhibits substantially stronger wind speeds and also highlights the prevailing west-south-westerly synoptic wind. The other stations are clearly more sheltered from the west and winds are more commonly channelled from the south or south-west. However, all stations show clear evidence of localised effects.

Tables 2 and 3 present comparisons between observations and mesoscale model forecasts of air temperature. Unsurprisingly, the model is unable to simulate the urban heat island effect, seen most clearly at the Guild Hall. At 12z the shorter range forecasts are more accurate than the longer-range ones at Guild Hall and Morriston, however this finding is not repeated at 00z.

Table 2: Bias of the 12z air temperature (°C) between Observations and Forecast data during 2005

	(Guild Hall – Forecast)	(Morriston – Forecast)	(Morfa – Forecast)
Observation – (T+6)	1.6	0.2	-1.7
Observation – (T+12)	2.0	0.5	-1.4
Observation – (T+24)	1.9	0.5	-1.4
Observation – (T+48)	2.1	0.7	-1.2
Observation – (T+72)	2.1	0.7	-1.2

Table 3: Bias of the 00z air temperature (°C) between Observations and Forecast data during 2005

	Guild Hall - Forecast	Morriston - Forecast	Morfa - Forecast
Observation – (T+6)	2.9	1.2	-1.1
Observation – (T+12)	2.7	1.0	-1.4
Observation – (T+24)	2.8	1.1	-1.2
Observation – (T+48)	3.0	1.2	-1.2
Observation – (T+72)	2.9	1.2	-1.2

Figure 3: 2005 Annual Wind Roses at the Guild Hall (top left), Morfa (top right), Morriston (bottom left) and Mumbles Head (bottom right).

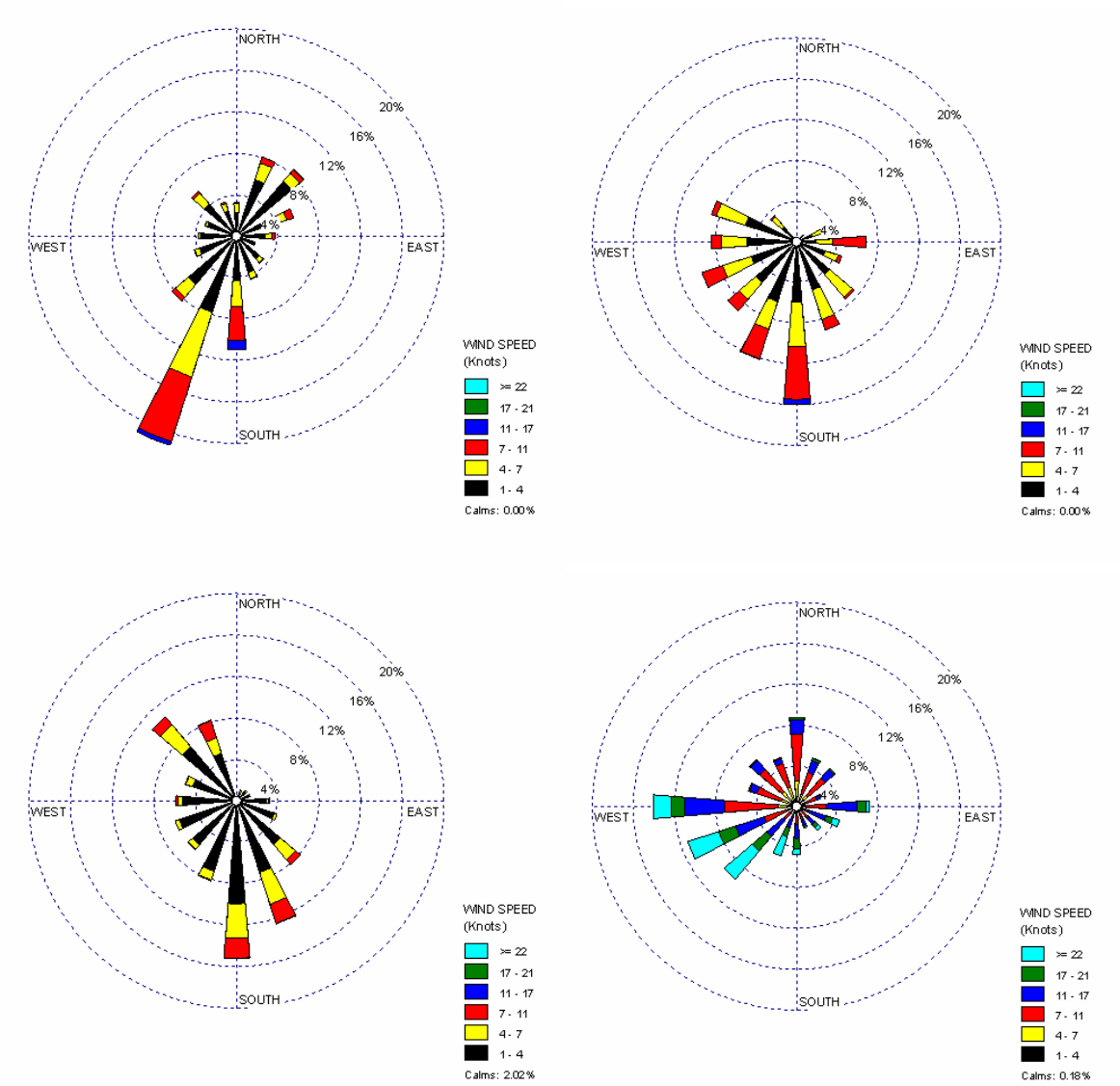

CONCLUSIONS

It is clear that the many different microclimates in and around a city make the choice of weather station data for urban air pollution modelling a difficult one; sensitivity tests are advised. Knowledge of bias in forecast data is also important in terms of the potential impact on model simulations and subsequent air quality management decision-making. We explore these points further on our poster.

ACKNOWLEDGEMENTS

We gratefully acknowledge the British Atmospheric Data Centre for meteorological data from the Mumbles Head synoptic weather station. We also thank the Saudi Cultural Bureau for funding this work.

IMPROVING THE MARTILLI'S URBAN BOUNDARY LAYER SCHEME: VALIDATION IN THE BASEL REGION

R. Hamdi[1], G. Schayes
Institut d'Astronomie et de Géophysique George Lemaître, University of Louvain,
B-1348 Louvain-la-Neuve, Belgium.
[1]present affiliation : Royal Meteorological Institute of Belgium, Uccle, Brussels, Belgium

ABSTRACT

Using the measurements obtained during the Basel urban boundary layer experiment (BUBBLE), a new version of the urban module of Martilli has been developed and implemented in the mesoscale model TVM. The improvements deal with a new form of the cross canyon drag, an additional along canyon drag and the taking into account of the urban vegetation cover. Being first run on 1-D column, the results show a better reproduced wind speed profile for along and cross canyon flow. The simulated canyon air temperature is also improved when we take into account the urban vegetation and the model partitions the surfaces energy fluxes appropriately.
The model has also been run in 3D mode around the Basel region using the perturbation version of TVM. The results show better agreement of the improved model with the observations on a statistical basis.

1. INTRODUCTION

Numerous investigations have shown that buildings and urban land use significantly modify the micro and mesoscale flow fields. Since mesoscale models do not have the spatial resolution to simulate the fluid dynamic and thermodynamic in and around urban structures, an urban canopy parameterization is used to represent the drag, heating, radiation attenuation, and enhanced turbulent mixing produced by the sub-grid scale urban elements. The parameterisation used here, which has been described in Martilli et al. (2002), combines the thermal and dynamical effects of the urban canopy. The thermal part of the parameterisation of Martilli et al. (2002) has already been validated with measurements from two mid-latitude European cities (Hamdi and Schayes, 2005). However, analysing the paper of Roulet et al. (2004) one can see that, even if the main dynamical effects of the urban canopy are reproduced, comparison with measurements seem to indicates that some physical processes are still missing in the parameterisation. In most of the cases, the model still overestimates the wind speed inside the canopy layer and it can have difficulties to simulate the maximum of the friction velocity which appears above the buildings roofs. Therefore, a new version of the urban module of Martilli has been developed in this study taking into account of the urban vegetation cover and a new drag formulation. This new version is implemented in the mesoscale model TVM **(**Topographic Vorticity-mode mesoscale model**)**. The goal of the present study is to validate this new version of the urban module using data from the BUBBLE (Basel urban boundary layer experiment) campaign carried out in the city of Basel, Switzerland.

2. URBAN AREA CHARACTERISTICS AND MEASUREMENTS

As a part of the BUBBLE measurements (Rotach et al., 2005) in 2001/2002 in the city of Basel, two micro-meteorological towers were operated in dense urban areas over 9 and 11 months (Basel-Sperrstrasse and Basel-Spalenring see Fig. 1): (i) Basel-Sperrstrasse (U1), this site is located in a heavily built-up part of the city ("European urban", dense urban, mainly residential 3 to 4 storey buildings in blocks, flat commercial and light industrial buildings in the backyards). The measurements set up consists of a tower inside a street canyon reaching up to a little more than two times the building height, where six ultrasonic anemometer-thermometers and full radiation component measurements are installed. (ii) Basel-Spalenring (U2), is located in the western part of the city of Basel in an area with a slightly different building structure and especially more trees than Basel-Sperrstrasse. The site is equipped with a micro-meteorological tower, reaching up to approximately two times the building height, including a profile of six ultrasonic anemometer-thermometers and full radiation component measurements. The profile is divided into a canyon part within alley trees (A to C) and a tower part that is shifted toward the backyard (D to F).

3. NEW VERSION OF THE URBAN MODULE

- *Introduction of the fraction of vegetation:* The principle of the urban surface exchange parameterisation of Martilli, is that extra terms are added to the momentum, heat, and turbulent kinetic energy equation separately. These terms are taken into account in proportions to the area of the surface fraction of three urban surface types: street, wall, and roof. So, no moisture flux is allowed in the urban canyon. However, in the literature a lot of numerical simulations and fields measurements indicate that increasing vegetation cover can be effective in reducing the surface and air temperature near the ground. In order to

take into account the vegetation effect on urban canopy, we divide the urban grid cell into an non-urban

(a) U1 (b) U2

Fig. 1. The instrumentation tower at urban area (a) Basel-Sperrstrasse and (b) Basel-Spalenring.

fraction (vegetated fraction in %) and an urban fraction, and then further subdivide the urban canopy fraction into street, wall, and roof according to Martilli's scheme.

- *Introduction of a new lateral friction:* In the urban module of Martilli, the force induced by the presence of the building is orthogonal to the street canyon. The effect of the flow parallel to the street canyon is not taken into account. In order to correct this, we partition the overall force imparted to a roughened surface by a fluid passing over it, into the force exerted on the roughness elements and the force exerted on the intervening wall surface (East and West wall).
- *New drag formulation:* Analysing the results of the BUBBLE campaign, we found that the drag coefficient for cross canyon flow increases with height inside the street canyon. However, in the urban module of Martilli, the drag coefficient is kept constant at every level inside the street canyon. So, in order to reproduce the observed effect of the augmentation of the drag coefficient in the urban module, a new drag formulation is adopted in which we calculate at every level inside the street canyon the sum of the drag force calculated for this level and the cumulated drag force calculated below.

4. VALIDATION IN 1-D

In this study, TVM is run on a vertical column using measurements at 30 m and 38 m, respectively for the two towers U1 and U2, as forcing. The period of the simulation extends from 16 June to 30 June 2002 and corresponds to the first half of the IOP in the frame of the BUBBLE campaign. This period is a unique opportunity, firstly, to quantify the impact of the urban exchange parameterisation on meteorological modelling and secondly to investigate its results over completely different urban surfaces under the same synoptic forcing. Three simulations were performed. The first simulation, denoted *"urban"*, uses the initial urban version of TVM. The second simulation, called *"Imp-urban"*, uses the improved urban version of TVM. The third simulation, called *"class"*, represents the classical approach, using Monin-Obukhov similarity theory, used in TVM to account for urban surface (city characterised only by a change in roughness length and the surface conditions).

Because the profile of wind speed shows a strong dependence on wind direction relative to the canyon alignment, two flow patterns are distinguished:

- Along canyon flow with the mean wind within 10° of the canyon direction.
- Cross canyon flow with the mean wind within 10° perpendicular to the canyon direction.

The fig. 2 presents the median profile of the wind speed normalised by u(top) at the tower top for cross canyon (left) and along canyon flow (right), and for the two urban sites **U1** (top) and **U2** (bottom). Calm situations with a mean wind speed lower than 1 m s^{-1} at top level are excluded.

- **Cross canyon flow**

For cross canyon flow (Fig. 2a and Fig. 2c), the new simulation *"Imp-urban"* fits much better to the observations, especially inside the street canyon where the nearly constant wind profile is well reproduced for U1. For U2 the simulated drag force inside the street canyon is still underestimated.

- **Along canyon flow**

The profile of wind speed for along canyon flow (Fig. 2b and Fig. 2d) is well reproduced especially inside the street canyon where a nearly linear wind profile is observed for U1. For U2 the simulated drag force inside

the street canyon is still underestimated. Above roof level the *"Imp-urban"* simulation reproduces very well the observed profile.

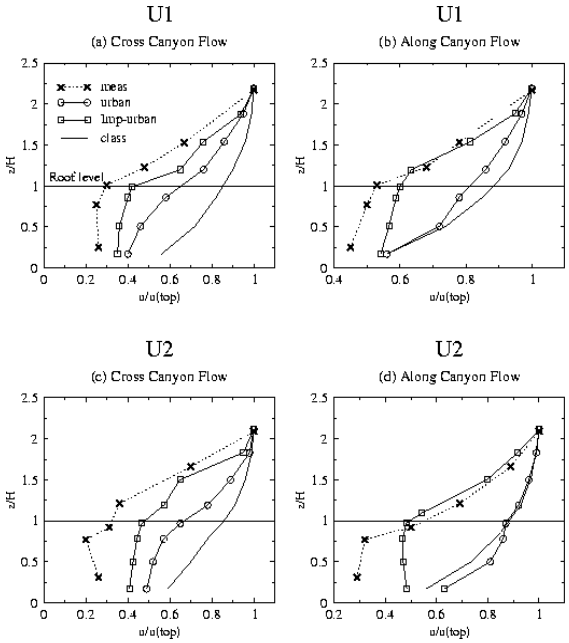

Fig. 2. The median profile of wind speed normalised by u(top) at the tower top for cross canyon flow (left) and along canyon flow (right), and for the two urban sites U1 (top) and U2 (bottom) during the first half of the IOP in the frame of BUBBLE for "Imp-urban", "urban", "class", and measurements.

In order to validate the urbanised version of TVM for temperature, two clear sky days are chosen: June 17 and June 18. Apart from the *"class"* and *"Imp-urban"* simulation, with the new version of the urban module of Martilli, a third urban simulation, denoted *"urban-0%"*, was performed for U2, with the vegetated fraction equal to 0%.

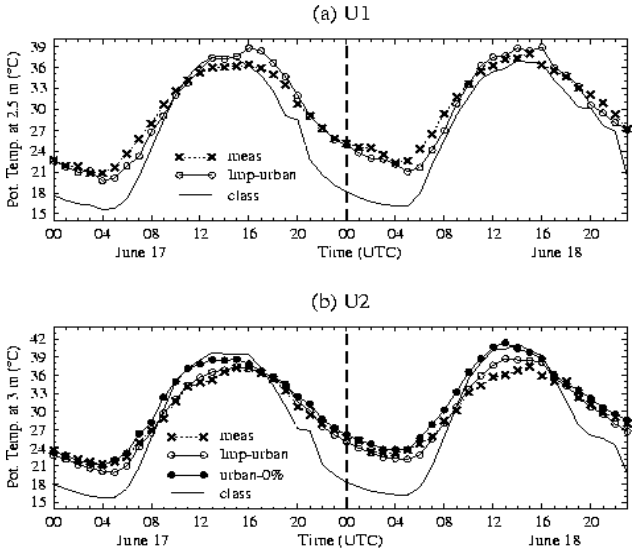

Fig. 3. Time variation of potential temperature, from June 17 to June 18 inside the street canyon at 2.5 m for U1 (top) and 3 m for U2 (bottom), observed and computed with the *"Imp-urban"* and the *"class"* simulation. For U2 a third simulation called *"urban-0%"* with the vegetated fraction equal to 0 % has been computed.

Good correlations are found between the *"Imp-urban"* simulations and the observations for both sites. However, the *"urban-0%"* simulation overestimates the average daily maximum temperature by 3 °C for U2. This is mainly due to the omission of the passive cooling effect of the vegetation in daytime, which leads to a serious overestimation of the air temperature especially for U2 where there are trees inside the street canyon (see Fig. 1b). The *"Imp-urban"* simulation taking into account the vegetated fraction of every site seems to fit better to the observations during daytime. In fact, the overestimation of the average daily maximum temperature is reduced to 1 °C for U2. This overestimation is probably due to an overestimation of the heat

flux from the street surface, this cannot be confirmed, as no measurements has been taken in the first 3 meters of the street canyon. Cooling during night-time is less important with the urban simulation than with the classical one. As a result, the classical simulation underestimates the daily minimum by 3 to 5 °C.

5. VALIDATION OVER THE BASEL REGION IN 3-D

In the 3-D validation, we compare model results with data from 6 stations representing three types of land use (urban: U, suburban: S, rural: R): U1, U2, S1, R1, R2, and R3. The largest differences between the urban and classical simulations are computed at night for the stations located in the downtown areas (see Fig. 4). At the urban sites (U1, U2), temperatures computed by "urban" are in quite good agreement with measurements. The improvements in the urban simulation are related to the sources of energy and the trapping of radiation in urban areas which reduce the nocturnal cooling. However, the urban simulation has a tendency to produce higher maximum temperature than observed in U1, U2, and S1. The temperatures data from station U1 were best reproduced by "urban", according to the root-mean-square differences between simulated and experimental values calculated for the three days covering the period of simulation.

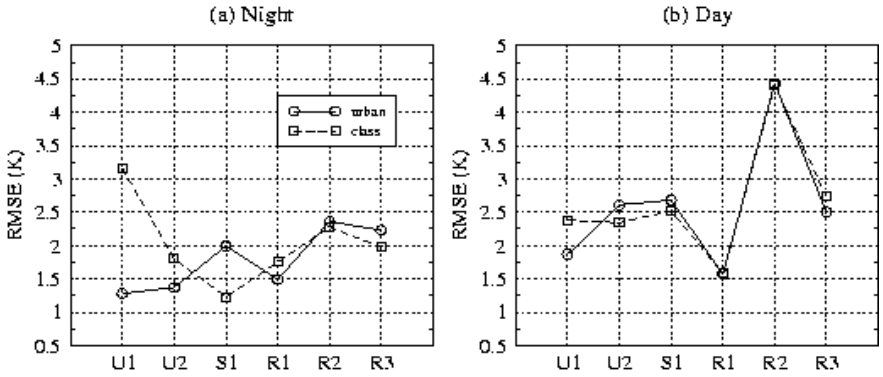

Fig. 4. The average daytime/night-time RMSE (K) of air temperature at U1, U2, S1, R1, R2, and R3 from June 25 to June 27, according to the "urban", and "class" simulations. Daytime values are averaged from 0600 to 2000 UTC, nocturnal values from 2100 to 0500 UTC.

6. CONCLUSION

In this work, some improvements have been brought to the urban scheme of Martilli : the introduction of the fraction of vegetation present in the urban canopy, the introduction of a new lateral friction to take into account the friction during along canyon flow and a new drag formulation for calculating the effect of high building on the flow. These modifications allowed a significant better reproduction of the measured wind and temperature vertical profiles.

7. ACKNOWLEDGEMENTS

Thanks to A. Martilli for providing us the code of his urban boundary layer scheme. The parameterization of Martilli is obtained in the frame of the EU-FUMAPEX project. The authors are very grateful to A. Christen for providing the BUBBLE database. Many thanks go to A. Clappier, Y.-A. Roulet, and C. Muller who provided assistance.

8. REFERENCES

Hamdi, R. and Schayes, G. 2005. 1-D validation of the Martilli's urban boundary layer scheme with measurements from two mid-latitude European cities. ACPD 5, 4257-4289.

Martilli, A., Clappier, A. and Rotach, M.W. 2002. An urban surface exchange parameterisation for mesoscale models. Boundary-Layer Meteorology 104 261-304.

Rotach, M.W. et al.. 2005. BUBBLE: a Major Effort in Urban Boundary Layer Meteorology, Theoretical Applied Climatology, In press.

Roulet, Y.A., Martilli, A., Rotach, M.W. and Clappier, A. 2004. Validation of an urban surface exchange parameterisation for mesoscale models-1D case in a street canyon, Journal of Applied Meteorology accepted.

EVALUATION OF THE PBL MODEL YORDAN WITH COPENHAGEN DATA FOR APPLICATION IN AIR POLLUTION MODELING

M. Kolarova[1]*, D. Yordanov[2], D. Syrakov[1], T.Tirabassi[3], U. Rizza[4], and C. Mangia[4]

[1] *National Institute of Meteorology and Hydrology (NIMH) - BAS, Sofia, BULGARIA*
[2] *Institute of Geophysics - BAS, Sofia, BULGARIA*
[3] *ISAC, CNR, Bologna, ITALY*
[4] *ISAC, CNR, Lecce, ITALY*
*(*M. Kolarova[1] - Author for correspondence, e-mail Maria.Kolarova@meteo.bg)*

ABSTRACT
Evaluation of eddy diffusivity and wind parameterisations schemes with Copenhagen data set is performed applying the PBL model YORDAN based on the similarity theory. The turbulent parameterisations have been included in an advanced operative dispersion model – VHDM, and evaluated against the Copenhagen data seta. The YORDAN model is used for simulation of the ground-level cross-wind concentration applying the VHDM model with two different parameterisations for the wind and k- profiles. The input data for the PBL model YORDAN are defined by the Monin-Obukhov length scale and the friction velocity taken from the experimental data. The results obtained can be used as a verification of the models and show the applicability of YORDAN model in air pollution simulations.

1. INTRODUCTION
Most of air quality dispersion models used for regulatory applications is based on K-diffusion formulations. The reliability of the K-approach strongly depends on the way the wind and eddy diffusivity are determined on the basis of the turbulence structure of the PBL and on the model ability to reproduce experimental diffusion data.
The aim of this paper is to evaluate the PBL parameterisation developed by Yordanov et al., (1983; 1997; 1998) using the dispersion model VHDM and applying Copenhagen data set.
The model VHDM (Virtual Height Dispersion Model) is an operative model for evaluating ground-level concentration from elevated sources (Tirabassi and Rizza, 1994).
The PBL model YORDAN, calculates the wind and eddy diffusivity profiles in the PBL under different stability conditions based on Monin-Obukhov similarity theory. In this paper the *k* and wind profiles in PBL are obtained from the surface turbulent fluxes, defined by the Monin-Obukhov length scale (L) and the friction velocity (u_*), taken from the experimental data, applying YORDAN model.

2. THE PBL MODEL YORDAN
The simple two-layer model described in Yordanov et al. (1983) is used to produce the vertical profiles of the wind and the vertical turbulent exchange coefficient. The PBL model consists of a Surface Layer (SL) with height h_* and an Ekman layer above it.

In the SL, $z \le h_*$, the wind profile is determined as:

$$\kappa\frac{\bar{u}(z)}{u_*}=\begin{cases}\ln(z/z_0)+10\zeta & \zeta\ge\zeta_0 \quad \mu\ge 0\\ \ln(z/z_0) & -0.07\le\zeta\le\zeta_0 \quad \mu<0\\ \ln(-0.07/\zeta_0)+3\left[1+(0.07/\zeta)^{1/3}\right] & \zeta\le -0.07 \quad \mu<0\end{cases} \qquad (1)$$

where $\mu=\dfrac{\kappa\, u_*}{fL}$ is the internal stratification parameter, κ = 0.4 is the von Karman constant, $\zeta = z/L$ is the non-dimensional height, $\zeta_0 = z_0/L$ is the non-dimensional roughness, and f is the Coriolis parameter ($f=10^{-4}\,s^{-1}$).

For the non-dimensional SL height $h(\mu)$ the following relations are used:

$$h(\mu)=\begin{cases}0.28/\mu, & \mu\ge 9.2\\ 0.03, & -9.2<\mu<9.2\\ 0.01|\mu|^{1/2}, & \mu\le -9.2\end{cases} \qquad (2)$$

For the non-dimensional turbulent exchange coefficient K_m we have:

$$K_m=\begin{cases}Z/(1+10\mu Z), & Z_0\le Z\le h, \quad \mu\ge 0\\ Z, & Z_0\le Z\le(-0.07/\mu), \quad -9.2<\mu<9.2.\\ (-0.07/\mu)^{-1/3}Z^{4/3}, & (-0.07/\mu)\le Z\le h, \quad \mu\le -9.2\end{cases} \qquad (3a)$$

For the dimensional turbulent exchange coefficient for momentum we use the relation:

$$k_z = (\kappa^2 u_*^2 / f)\, K_m \qquad (3b)$$

Here, we use the following relations: $h = h_* / H$ is the non-dimensional SL height, $H = \kappa u_* / f$ is the height scale, $Z = z / H$ is the non-dimensional height, and $Z_0 = z_0 / H$ is the non-dimensional roughness. We can notice that $h = h_*\, f / \kappa u_*$ and from it we obtain for the dimensional SL height the relation: $h_* = h\, \kappa u_* / f$.

In the Ekman layer (*Z*>*h*), the turbulent exchange coefficient is assumed not to change with height and to be equal to K_{mh}, i.e. following (5) we obtain:

$$K_{mh} = \begin{cases} h/(1+10\mu h), & \mu \geq 0 \\ h\ , & -9.2 < \mu < 9.2\ . \\ (-0.07/\mu)^{-1/3} h^{4/3}, & \mu \leq -9.2 \end{cases} \qquad (4a)$$

Here the dimensional turbulent exchange coefficient for momentum is the obtained by the relation:

$$k_z = k_{zh} = (\kappa^2 u_*^2 / f)\, K_{mh} \qquad (4b)$$

The velocity components u and v at height z are calculated from the relations:

$$u = |v_g| \cos\alpha + P \frac{u_*}{\kappa} \qquad \text{and} \qquad v = |v_g| \sin\alpha + Q \frac{u_*}{\kappa}, \qquad (5)$$

where α is the cross-isobaric angle, u_g, v_g are the geostrophic wind velocities components, and the non-dimensional velocity defects *P* and *Q* are given by the following expressions:

in SL:

$$P = \begin{cases} \ln(Z/h) + 10\mu(Z-h) - (2K_m)^{-1/2}, & Z_0 \leq Z \leq h, \quad at\ \mu \geq 0 \\ \ln(-\mu Z/0.07) - 3\left[1 - (-0.07\, h/\mu)^{1/3}\right] - (2K_m)^{-1/2}, & Z_0 \leq Z \leq (-0.07/\mu), \\ -3\left[(-0.07\, Z/\mu)^{1/3} - (-0.07h/\mu)^{1/3}\right] - (2K_m)^{-1/2}, & (-0.07/\mu) \leq Z < h, \end{cases} \quad \mu < 0 \qquad (6a)$$

and above SL:

$$P = -\exp(-\psi)\left[\cos\psi - \sin\psi\right]/(2K_{mh})^{1/2}, \qquad at \quad Z \geq h\ , \qquad (6b)$$

and for the velocity defect in vertical direction we have:

$$Q = \begin{cases} (2K_m)^{-1/2}, & at \quad Z \leq h \\ \exp(-\psi)(\cos\psi + \sin\psi)/(2K_{mh})^{1/2}, & at \quad Z > h \end{cases}. \qquad (7)$$

In Eq. (6b) and Eq. (7) $\psi = (Z-h)/(2K_{mh})^{1/2}$, and the x-axis is directed along the surface wind. Replacing the expressions from Eq. (6) and (7) in Eq. (5) we can find the velocity profiles given by the expression for the mean wind:

$$\bar{u}(z) = |u| = \sqrt{u^2 + v^2}\ . \qquad (8)$$

In the present paper the PBL model Yordan is used starting from the experimental data for *L* and u_* and applying the approach "bottom-up" described by Yordanov et al. (2003).

3. VHDM AIR POLLUTION MODEL

The virtual height dispersion model (VHDM) is an operative short range model for evaluating ground level concentration from industrial sites. It approximates the cross-wind integrated ground level concentration $C_y(x,0)$ by means of a Fickian- type formula in which the real source is replaced by a virtual source placed at the geometric average of the two virtual source heights μ_s and ς_s function of the wind speed and eddy diffusivity profile:

$$C_y(x,0) = \frac{Q}{\sqrt{\pi \cdot x \cdot \bar{u}_s \cdot k_s}}\, e^{\left(-\varsigma_s \mu_s / (4xk_s / \bar{u}_s)\right)} \qquad (9)$$

where *Q* is the source strength, $\bar{u}_s$ and k_s are the wind speed and the eddy diffusivity at the source height respectively, μ_s and ς_S are two virtual source heights expressed by simple functions of the vertical profiles of wind and turbulent diffusivity defined as:

$$\mu_s = \int_{z_o}^{H_s} \left(\frac{\bar{u}(z)}{k_z(z)} \frac{k_s}{\bar{u}_s} \right)^{1/2} dz \,, \qquad \zeta_s = \int_{z_o}^{H_s} \frac{\bar{u}(z)}{\bar{u}_s} dz \tag{10}$$

where H_s is the effective release height.

The model accepts both experimental and theoretical profiles for the eddy diffusivity $k_z(z)$ and for the wind velocity $\bar{u}(z)$, provided by the integrals in Equation (10). Lupini and Tirabassi (1981) shown that the ground level concentrations admit a lower and upper bound that represent solutions at the ground level of two diffusion equations of Fickian-type with the two virtual sources μ_s and ζ_s respectively.

Here the interpolation between the two bounds is used and the selected above Gaussian formula, since the predicted maximum position (x_m): $x_m = \frac{\bar{u}_s \zeta_s \mu_s}{2k_s}$ (11) is exactly the same as that predicted by the solution of the advection-diffusion equation, which admits power law profiles of wind and eddy diffusivity coefficients (Tirabassi, 1989).

4. COMPARISON WITH EXPERIMENTAL DATA

We evaluated the performance of the PBL parameterization, applying the VHDM air pollution model to the Copenhagen data set (Gryning and Lyck, 1984; Gryning and Lyck, 2002). The meteorological conditions during the dispersion experiments, ranged from moderately unstable to convective.

Table 1 summarises the meteorological data during the Copenhagen experiment used as input data for the PBL models simulations. U_s is the wind speed at the source height, w_* is the convective velocity scale and $\mu_c = z_i / L$ is the internal stratification parameter for convective condition.

Table 1. The meteorological data observed during the Copenhagen experiment used in the simulations.

Experiment	Us m/s	u_* m/s	L m	w_* m/s	z_i m	$\mu_c=z_i/L$
1 - Sept. 20 1978	3.4	0.36	-37	1.7	1980	-53.5
2 – Sept. 26 1978	10.6	0.73	-292	1.8	1920	-6.6
3 – Oct. 19 1978	5.0	0.38	-71	1.3	1120	-15.8
4 – Nov. 3 1978	4.6	0.38	-133	0.7	390	-2.9
5 – Nov. 9 1978	6.7	0.45	-444	0.7	820	-1.8
6 - April 30 1979	13.2	1.05	-432	2.0	1300	-3.0
7 – June 27 1979	7.6	0.64	-104	2.2	1850	-17.8
8 – July 6 1979	9.4	0.69	-56	2.2	810	-14.5
9 - July 19 1979	10.5	0.75	-289	1.9	2090	-7.2

4. 1. Evaluation of the parameterizations used

The wind speed and eddy diffusivity profiles, determined by the model YORDAN, are compared with the following wind profiles and turbulent exchange coefficients (Tirabassi and Rizza, 1994) derived from literature and largely used in dispersion models according (Pleim and Chang, 1992).

Wind profile

The wind velocity profile used has been parameterised as follow:

For an unstable PBL ($L < 0$)

$$\bar{u}(z) = \frac{u_*}{\kappa} \left[\ln(z/z_0) - \Psi_m(z/L) + \Psi_m(z_0/L) \right] \tag{12}$$

Ψ_m is a stability function given by:

$$\Psi_m = 2\ln\left[\frac{1+A}{2}\right] + \ln\left[\frac{1+A^2}{2}\right] - 2\tan^{-1}(A) + \frac{\pi}{2} \,, \tag{13}$$

with $A = (1 - 16z/L)^{1/4}$.

For a stable PBL (L>0) we use the relations:

$$\bar{u}(z) = \frac{u_*}{\kappa} \left[\ln(z/z_0) + \Psi_m(z/L) \right], \tag{14}$$

where the function Ψ_m is given by the expression:

$$\Psi_m(z/L) = 4.7\,(z/L) \,. \tag{15}$$

Eddy diffusivity

Following Pleim and Chang (1992) during stable and neutral conditions at $z_i / L \geq -10$:

$$k_z = \kappa u_* z(1 - z / z_i)^2 / \phi_h \quad (16)$$

where:

$$\phi_h = 1 - 5\left(\frac{z}{L}\right). \quad (17)$$

During convective conditions at $z_i / L \leq -10$ the friction velocity was replaced by the convective velocity scale w_* defined as $w_* = u_*\left(\frac{z_i}{-kL}\right)^{1/3}$ and the following relation is used:

$$k_z = \kappa w_* z(1 - z / z_i) \quad (18)$$

4.2. Results and discussion

In Figure 1 the observed and computed by the two models ground level concentrations as a function of the source distance are presented for each Copenhagen experiment. Model I refers to the PBL model Yordan, described in 2, where the mean wind is calculated according Eqs. (1) (5) and (8), the eddy diffusivity using Eqs. (3) and (4). Model II refers to Eqs. (12) and (14) for the wind profiles and for the eddy diffusivity Eqs. (16) and (18) are used. The surface cross-wind integrated concentrations are calculated with the model VHDM according Eq. (9), where the virtual height μ_s and ζ_s are calculated from Eq. (10) for Model I and Model II with the corresponding u and k – profiles described above.

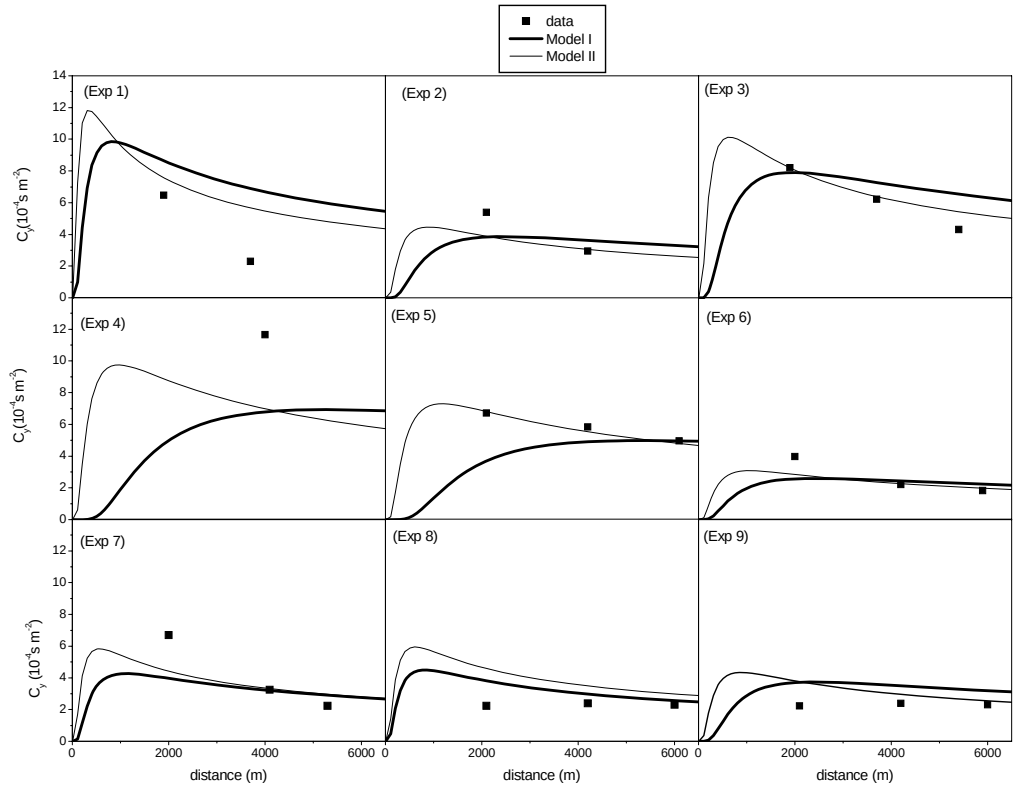

Figure 1 Comparison of ground level observed data with the cross-wind integrated concentration predicted by the models - function of the distance from the source *(MODEL I - YORDAN) and (MODEL II – VHDM)*

The main difference between the model results with the two parameterizations are close to the source where Model II gives higher concentration values. There are no big differences at higher distances from the source where the measurements are taken. So at least in the range of measurements the performances of the two models are quite similar.

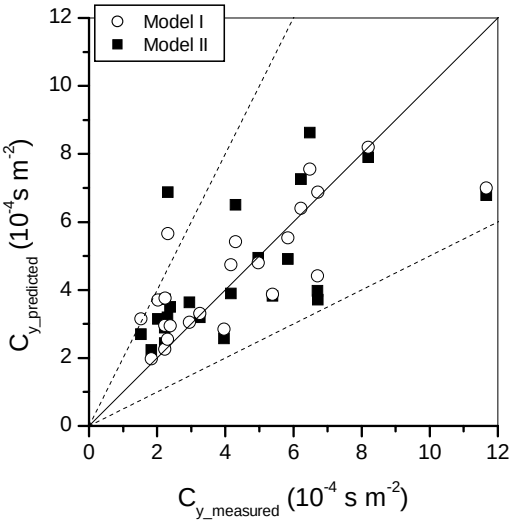

Figure 2 Copenhagen dataset. Scatter plot of observed versus predicted crosswind-integrated concentrations normalized with the emission source rate. Points between dashed lines are in a factor of two.

Figure 2 shows the observed and predicted scatter diagram of ground-level crosswind integrated concentrations using VHDM model with the two wind and eddy diffusivity profiles described above as Model I and Model II.

5. CONCLUSIONS

In this paper we present practical models, that accept that wind and eddy diffusivity profiles are functions of the height evaluating two different parameterization of wind and eddy diffusivity profile.
The parameters considered for the evaluation of the model performances are: mean wind and the vertical turbulent diffusion coefficient.
Different expressions of the vertical turbulent diffusion coefficient were used in VHDM model and in YORDAN model, together with different expressions for the calculation of mean wind.
The turbulent parameterisations have been included in an advanced operative model, and evaluated against the Copenhagen data seta. Analysis of results and the application of statistical indices show that model which included the eddy diffusivity parameterisation proposed, produces a good fit for the experimental ground level concentration data in the various stability regimes which identify the PBL.

Acknowledgements
The authors thank to S.-E. Gryning for the supplied results from the Copenhagen experiment. This paper was done under the bilateral colaboration between Italian CNR and Bulgarian Academy of Sciences (BAS).

REFERENCES

Gryning S.E. and E. Lyck, 1984: Atmospheric dispersion from elevated sources in an urban area: Comparison between tracer experiments and model calculations. *J. Climate Appl. Meteor.*, **23**, 651-660.

Gryning S.E. and Erik Lyck. (2002) RISO-R-1054 (rev.1) (En). The Copenhagen Tracer Experiment: Reporting of measurements, RISOE Nathional Laboratory, Roskilde, 2002.

Lupini R. and Tirabassi T. (1981) A simple analytic approximation of ground-level concentration for elevated line sources. *J. Appl. Meteor*., vol. 20, pp. 565-570.

Tirabassi T. (1989) Analytical air pollution advection and diffusion models. *Water, Air and Soil Poll.*, vol. 47, pp. 19-24.

Tirabassi, T. and Rizza, U. (1994) Applied dispersion modelling for ground-level concentrations from elevated dources, *Atmos. Environ.*, Vol. 28, pp. 611-615.

Yordanov, D., Syrakov, D., Djolov, G. (1983) A Barotropic Planetary Boundary Layer, *Boundary Layer Meteorology* **25**, 1-13.

Yordanov D., D. Syrakov, M. Kolarova, (1997) On the Parameterization of the Planetary Boundary Layer of the Atmosphere, The Determination of the Mixing Height -Current Progress and Problems. EURASAP Workshop Proc., 1-3 Oct. 1997.

Yordanov, D., Syrakov, D., Djolov, G. (1998) Baroclinic PBL model: neutral and stable stratification condition, *Bulg. Geophys. J*., **14**, No1-2, 5-25.

Yordanov D. L., Syrakov D. E., Kolarova M. P. (2003) Parameterization of PBL from the surface wind and stability class data, *Proc. of NATO ARW on Air Pollution Processes in Regional Scale*, Halkidiki, Greece, 13-15 June 2002, NATO Science Series, D. Melas and D. Syrakov (eds.), Kluwer Acad. Publ., Netherlands, Vol. 30, pp. 347-364.

Proceedings of the 6th International Conference on Urban Air Quality
Limassol, Cyprus, 27-29 March 2007

IMPLEMENTATION AND TESTING OF URBAN PARAMETERIZATION IN THE WRF MESOSCALE MODELING SYSTEM.

Alberto Martilli[1]
CIEMAT, Madrid, Spain.
Rainer Schmitz,
Universidad de Chile, Santiago, Chile.
Fernando Martin
CIEMAT, Madrid, Spain.

ABSTRACT
Buildings reduce wind speed and modify wind direction, increase turbulence, generate shadows and trap radiation. Different urban surfaces respond in a very different manner to the radiative forcing. Construction materials influence the way the heat produced within the buildings is transmitted to the atmosphere. Modeling such effects in details would require resolutions of the order of meters (the scale of the urban heterogeneity), which are impossible in mesoscale models. It is necessary, then, to parameterize such effects on average on the grid cell (usually of the order of one kilometer or several hundreds of meters). In this contribution, the implementation of an urban parameterization in the WRF (Weather Research and Forecasting) model is described. The urban parameterization accounts for the drag induced by the buildings, the turbulent effects, the trapping of radiation and shadowing in the canyon and the exchanges of heat between the interior and exterior of the buildings. The technique used in the implementation is presented, as long as bidimensional tests used to evaluate the capability of the model to reproduce the most important urban features known from literature.

1. INTRODUCTION

Numerical atmospheric models are increasingly used to simulate weather, air quality and local climatology over urban areas. The advantage of this kind of models is that, once they are validated against measurements for specific episodes, they can be used to evaluate possible future scenarios. For example, they can be used to evaluate the effectiveness of an abatement strategy for air pollution or a mitigation strategy of the Urban Heat Island (UHI) intensity. It must be remembered, moreover, that a city is a very complex system, and the different pieces of the problem are interconnected. For example, a planned change in urban structure to reduce the impact of the UHI (e. g. 'green' or 'white' roofs, or changes in the morphology of the city), alters the surface energy budget. As a consequence the whole structure of the urban boundary layer is affected (change in mixing height, temperature, urban breezes, etc.), and the dispersion of the pollutant is modified.

It is clear, then, that to reproduce these phenomena with the adequate accuracy, the numerical model must be able to reproduce the most important features of the urban boundary layer. The difficulty lies in the extreme complexity of the urban surfaces. As it has been demonstrated in several studies (for example, Rotach, 1993), in fact, the techniques developed for homogenous and flat surfaces (Monin-Obukhov Similarity theory, and one surface energy budget) fail to reproduce the atmospheric behavior over urban areas.

Main motivation of the present work is to implement a specific surface exchange parameterization for urban areas in the WRF modeling system. The expected outcome of the activity is a numerical mesoscale model that can be successfully used to help urban planners to evaluate the impact of the future city developments on air quality and microclimate.

In section 2 the WRF mesoscale model and the urban paramterization are shortly described, as well as the technique adopted in the implementation. In section 3, preliminary results are presented together with the problems encountered in the work. Section 4 is dedicated to the conclusion and future work.

2. METHODOLOGY

The Weather Research and Forecasting (WRF) is a next-generation mesocale numerical weather prediction system designed to serve both operational forecasting and atmospheric research needs (http://www.mmm.ucar.edu/wrf/users/) . It is the result of the collaboration between different institutions (among the others, NCAR, NOAA, NCEP). The WRF system has a variety of physical parameterizations, and two dynamics solvers: one called EM (Eulerian Mass), developed at NCAR, and one called NMM (Nonhydrostatic Mesoscale Model), developed at NCEP. In this study, the EM dynamical solver is used. This is justified because, as previously explained, the main objective is to improve the modeling

[1] CIEMAT, Edificio 70, p1.11. Avenida Complutense, 22. Madrid, Spain. E-mail: alberto.martilli@ciemat.es. Tel. ++34-913466299.

capabilities in the domain of air quality and local climatology. At the moment, in fact, only the version with the EM solver has a chemistry module embedded (WRF-Chem). It is expected, however, that the developments of the present work can be easily transferred to the NMM version, when needed.

The urban paramterization adopted is the one of Martilli et al. 2002. The parameterization takes into account the impact of the vertical (walls), and horizontal (streets and roofs) surfaces on the momentum and turbulent kinetic energy equations (mechanical factors), as well as on the temperature equation (thermal factors). For the mechanical part, a porous approach is used in analogy with the techniques used for vegetation canopy flows. For the thermal part, the heat fluxes from the vertical and horizontal surfaces are computed with an energy budget at the surface. The radiations needed for this budget take into account the shadowing, the reflections and trapping in the urban street canyons. Although more complex, this parameterization is more detailed than other schemes. Since the aim of the work is not the day-to-day forecast, rather the cases studies, the CPU constraints are less strict and the choice is justified. Moreover, the parameterization has been successfully tested over different cases both idealized and real with the mesoscale model FVM (Roulet et al. 2005, Martilli et al. 2003), and implemented in other models (AlMo). Since in the original version the urban parameterization was coupled with the turbulence scheme of Bougeault and Lacarrere (1989), this parameterization is also implemented in WRF. The nature of the coupling is in the introduction of source terms in the TKE equation within the urban canopy due to the presence of the buildings that increases the transformation of Mean Kinetic Energy into Turbulent Kinetic Energy, and the modification of the turbulent length scales to account for buildings effects.

From the technical point of view, the implementation has been carried out in the following way:

- For every grid point a percentage of urban area is defined.
- If the percentage of urban area in a grid point is greater than zero, then the model uses the urban parameterization to estimate the parameters a_ψ, b_ψ (where ψ can be the x or y component of the wind, the potential temperature or the TKE), that are needed to compute the tendencies (implicitly) in every layer within the urban canopy as:

$$\frac{\partial \Psi}{\partial t} = a_\psi \psi + b_\psi$$

  The modifications to the dissipation length scale due to the buildings are also estimated.
- The WRF surface routine for vegetated areas (NOAH, for example) is called to compute in the usual way the surface fluxes of momentum and heat.
- The a_ψ, b_ψ from the urban paramterization routine, and the surface fluxes from the vegetated areas, are then passed to the Boundary Layer routine where they are weighted based on the percentage of urban and rural areas present in the grid cell. In the same routine the vertical turbulent transport is computed, based on the Bougeault and Lacarrere, 1989, scheme. The total tendency due to both urban and rural effects, and turbulent transport is finally passed to the solver.

3. PRELIMINARY RESULTS

The new code has been tested over a 2-D flat terrain, with an idealized city in the center of the domain. The idea is to reproduce the base case simulation of Martilli, 2003. The resolution is 1km in the horizontal and about seven meters in the vertical close to the ground. The city is 10km wide, and the entire domain is 100km. The simulation starts at the 2000 LT, and run for 30 hours. Initial wind speed is 3 m s^{-1}. The urban data are the same as in Martilli, 2003. In the rural areas, the NOAH scheme is used with vegetation type grass, and soil moisture of 0.25.

Vertical profiles of real temperature at 0300 LT over the center of the urban areas, and over the rural area upwind the city, are presented in Figure 1. The model is able to reproduce a nocturnal urban heat island. The depth of the elevated inversion layer is about 60 meters, lower than the one simulated in Martilli, 2003. The reason of the weaker inversion layer is not clear, and may be linked with the differences in the rural areas that affects the stability of the approaching flow.

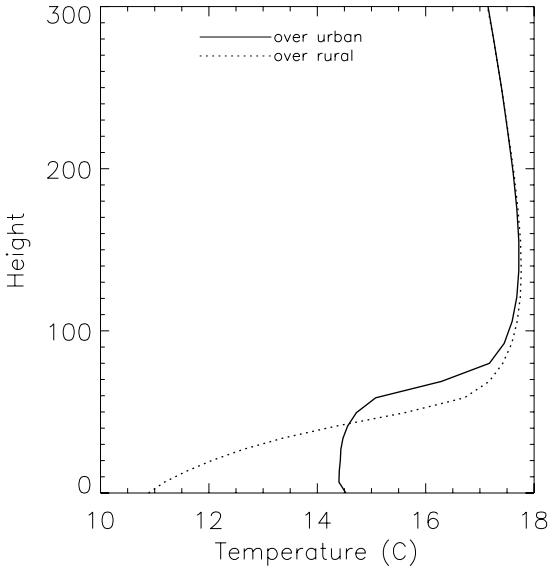

Figure 1. Vertical profile of real temperature over the center of the urban area (solid line), and over the rural area upwind of the city (dotted line).

During daytime, model is also able to reproduce an urban heat island, as it can be seen in the vertical section of potential temperature of Fig2a. The diurnal heat island seems weaker than the heat island modelled by Martilli, 2003. However, it is still able to induce an increase of wind speed above the city (Fig. 2b).

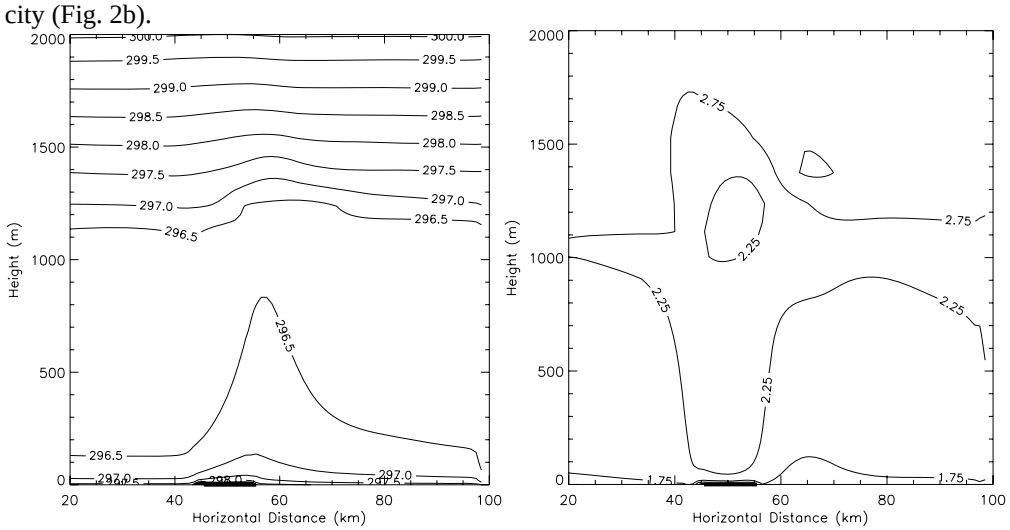

Figure 2. a) Vertical section of potential temperature field at 1200 LT (left panel), and b) horizontal wind speed (right panel). The city is located between km 45 and km 55 (thick line).

4. CONCLUSIONS.

An urban surface exchange parameterization has been implemented in the WRF mesoscale model and tested over a 2D domain. First results are encouraging since the new version of the code seems able to reproduce some of the most typical features of urban boundary layers. However several points of the implementation need to be clarified:

- The UHI intensity reproduced by the model seems to be weaker than the UHI intensity of previous studies with the same urban parameterization. The causes need to be investigated more deeply, to understand if it is linked with the urban parameterization itself, or, simply, with different conditions in the rural areas surrounding the city.
- The introduction of the drag term in the momentum equation can generate numerical instabilities. To avoid them in this study, an artificial horizontal diffusion of 1000 $m^2 s^{-1}$ has been added of. This approach is not very satisfactory, and a change in the numerical algorithm adopted in the implementation may improve the simulation.

5 . REFERENCES

P. Bougeault and P. Lacarrere, 1989. Parameterization of Orography-Induced Turbulence in a Mesobeta--Scale Model. Monthly Weather Review, **117**, 1872–1890.

Martilli, A., Clappier, A., and Rotach, M. W., 2002. An urban surface exchange parameterization for mesoscale models, Boundary-Layer Meteorol., **104**, 261,304.

Martilli, A., Y. A. Roulet, M. Junier, F. Kirchner, M. W. Rotach, and A. Clappier, 2003. On the impact of urban surface exchange paramterizations on air quality simulation: the Athens case. Atmospheric Environment, **37**, 4217-4231.

Martilli, A., 2003, Numerical Study of Urban Impact on Boundary Layer Structure: Sensitivity to Wind Speed, Urban Morphology, and Rural Soil Moisture, Journal of Applied Meteorology, **41**, 1247-1266.

Rotach, M. W., 1993. Turbulence close to a rough urban surface, Part I: Reynolds stress. Boundary-layer Meteorology, **65**, 1-28.

Roulet, Y. A., A. Martilli, M. W. Rotach and A. Clappier, 2005. Validation of an urban surface exchange parameterization for mesoscale models – 1D case in a street canyon. Journal of Applied Meteorology, **44**, 1484-1498.